Separation Science and Technology
Publication details, including instructions for authors and subscription information:
http://www.informaworld.com/smpp/title~content=t713708471

SEPARATION OF HYDROGEN ISOTOPES BY CHEMICAL ISOTOPE EXCHANGE IN SYSTEMS INVOLVING METAL AND INTERMETALLIC COMPOUND HYDRIDES

Boris M. Andreev[a]; Eldar P. Magomedbekov[a]
[a] Mendeleev University of Chemical Technology of Russia, Moscow, Russia

Online publication date: 30 July 2001

To cite this Article Andreev, Boris M. and Magomedbekov, Eldar P.(2001) 'SEPARATION OF HYDROGEN ISOTOPES BY CHEMICAL ISOTOPE EXCHANGE IN SYSTEMS INVOLVING METAL AND INTERMETALLIC COMPOUND HYDRIDES', Separation Science and Technology, 36: 8, 2027 — 2086
To link to this Article: DOI: 10.1081/SS-100104766
URL: http://dx.doi.org/10.1081/SS-100104766

SEPARATION SCIENCE AND TECHNOLOGY, 36(8&9), 2027–2086 (2001)

SEPARATION OF HYDROGEN ISOTOPES BY CHEMICAL ISOTOPE EXCHANGE IN SYSTEMS INVOLVING METAL AND INTERMETALLIC COMPOUND HYDRIDES

Boris M. Andreev* and Eldar P. Magomedbekov

Mendeleev University of Chemical Technology of Russia,
9 Miusskaya Square, Moscow 125190, Russia

ABSTRACT

This article reviews and analyzes the results obtained by studying isotope effects and kinetics of isotope exchange in systems involving heavy hydrogen isotopes and intermetallic compound hydrides for the last 20 years. Particular attention is paid to the analysis of possibilities to realize the separation process in the hydrogen-hydride phase systems. It is shown that hydrides of metals and intermetallic compounds represent suitable systems for solution of a number of hydrogen isotope separation problems, particularly for separation of tritium-containing gaseous mixtures. This article considers also the data on isotope effects, the rates of isotope exchange, and optimization of conditions for hydrogen isotope separation by using metal and intermetallic compound hydrides.

*Corresponding author.

INTRODUCTION

The systems involving heavy hydrogen isotopes and hydride phases of transition metals or intermetallic compounds (IMC) are characterized by large isotope effects, which can be used for separation of hydrogen isotopes. Many problems arising at nuclear fuel plants, such as recovery, purification, and storage of heavy hydrogen isotopes in tritium-containing systems of a thermonuclear reactor, extraction and separation of tritium from heavy water and some others, can be solved by using hydride-forming metals and IMC. Information on the interaction of heavy hydrogen isotopes with transition metals and IMC is limited and unsystematic, however, it enables consideration of a diversity of theoretical problems.

The theoretical aspects of interaction of heavy hydrogen isotopes with metals and IMC and systematic analysis of isotope equilibrium and kinetics of hydrogen isotope exchange in systems involving hydride phases have not been described so far in monograph literature. This article is targeted to fill this gap. During the preparation of the manuscript, we used both the data known from the literature and, primarily, the results of our own theoretical and experimental investigations performed during the last 20 years.

THERMODYNAMIC ISOTOPE EFFECT

Thermodynamic isotope effect, which is observed in hydrogen-hydride phase systems, is associated with the difference in isotherms of hydrogen sorption by the solid phase. Unlike well-known phase equilibrium in liquid-vapor systems, in metal-hydrogen systems the pressure and the temperature are independent parameters of sorption equilibrium and separation factor α can depend on the amount of sorbed gas. This requires the introduction of a differential separation factor characterizing separation of isotopes within a given part of sorption isotherm of sorption, which can be defined as follows (1,2):

$$\alpha_{\text{dif}} = (P_1/P_2)_n \tag{1}$$

where P_1 and P_2 are the equilibrium pressures of pure components over a sorbent at equal fillings (loadings) n.

Considering the filling for all previous parts of the isotherm, including the given one, and taking into account that hydrogen sorption is followed by its dissociation to atoms, the following expression for the separation factor can be derived:

$$\ln \alpha^0_{\text{A}-\text{B}} = \left(\frac{1}{2n}\right)\int_0^n \ln \alpha_{\text{dif}}\, dn = \left(\frac{1}{2n}\right)\int_0^n \ln(P_1/P_2)_n\, dn \tag{2}$$

where $\alpha^0_{\text{A–B}}$ is the separation factor at equal ratio of hydrogen isotopes A and B (e.g., H and D) in the gas phase.

MARCEL DEKKER, INC.
270 Madison Avenue, New York, New York 10016

Equation (2) can be used to calculate α values from experimentally determined isotherms by graphical integration. If the analytical expressions describing sorption isotherms are available the calculation of α is simplified due to the possibility of calculating the integral standing in Eq. (2).

Calculation of Separation Factor by Using Harmonic Oscillator Model

Besides experimental determination and calculation from sorption isotherms, the α values can also be computed by using the quantum-statistical method. Let us consider the isotope exchange of gaseous hydrogen with hydride phase as a conventional reaction of chemical isotope exchange

$$2A(Me) + B_2 \leftrightarrow 2B(Me) + A_2 \tag{3}$$

Then, the equilibrium constant of reaction (3) can be expressed as follows:

$$K_{A-B} = \frac{Z_{A_2}}{Z_{B_2}} \cdot \frac{Z^2_{B(Me)}}{Z^2_{A(Me)}} \tag{4}$$

where Z_{A_2} and Z_{B_2} are the sums over states of hydrogen molecules containing light and heavy isotopes, respectively (e.g., for H-T isotope exchange this means Z_{H_2} and Z_{T_2}), $Z_{A(Me)}$ and $Z_{B(Me)}$ are the sums over states of hydride phases of metal or IMC phase including light and heavy hydrogen atom (for the above example, $Z_{H(Me)}$ and $Z_{T(Me)}$).

Substitution of K in Eq. (4) by the known relation between K and α (3,4)

$$\alpha^0_{A-B} = (K_{A-B})^{1/2} \tag{5}$$

gives the following equation:

$$\alpha^0_{A-B} = (Z_{A_2}/Z_{B_2})^{1/2} \cdot (Z_{B(Me)}/Z_{A(Me)}) \tag{6}$$

The peculiarity of hydrogen isotopes consists in their non-equiprobable distribution in the reactions of homomolecular isotope exchange (HMIE) for example: $H_2 + D_2 = 2HD$ (characterized by the equilibrium constant K_{HD}) or in general form:

$$A_2 + B_2 = 2AB,\ K_{AB} \tag{7}$$

This results in inequality $Z_{A_2}/Z_{AB} < Z_{AB}/Z_{B_2}$, whereas for diatomic molecules that do not contain hydrogen the following equalities are rigorously obeyed:

$$Z_{A_2}/Z_{AB} = Z_{AB}/Z_{B_2} = (Z_{A_2}/Z_{B_2})^{1/2} \tag{8}$$

As deviation from equalities (8) in systems with molecular hydrogen leads to the appearance of concentration dependence of the separation factor (see be-

MARCEL DEKKER, INC.
270 Madison Avenue, New York, New York 10016

low), it is useful to distinguish the processes of isotope exchange in different ranges of concentrations of heavy isotope B. Thus, at low and high content of B in the mixture, the exchange reactions can be written as follows:

$$\text{Low:} \quad A(Me) + AB = B(Me) + A_2 \tag{9}$$

$$\text{High:} \quad A(Me) + B_2 = B(Me) + AB \tag{10}$$

Calculation of the sums over states for isotopic species of molecular hydrogen was performed by Bron et al. (5). A number of publications (4,6–15,17–22) report a moderate agreement of experimentally determined α values for a wide temperature range (195–353 K) with the values computed by the quantum-statistical method with the use of the three-dimensional harmonic oscillator model (HOM) for the hydride phase. According to the model, the ratio of sums over states of heavy and light hydrogen isotopes in the crystal lattice of metal or IMC is connected with frequencies of 3-fold degenerated atom modes ω_A and ω_B by the following equation:

$$\frac{Z_{B(Me)}}{Z_{A(Me)}} = \left[\frac{1 - \exp(-\hbar\omega_A/kT)}{1 - \exp(-\hbar\omega_B/kT)} \cdot \exp(\hbar(\omega_A - \omega_B)/2kT\right]^3 \tag{11}$$

or

$$\frac{Z_{B(Me)}}{Z_{A(Me)}} = \left[\frac{\sinh(u_A/2)}{\sinh(u_B/2)}\right]^3 \frac{Z_{B(Me)}}{Z_{A(Me)}} = \left[\frac{\sinh(u_A/2)}{\sinh(u_B/2)}\right]^3 \tag{12}$$

where $U_A = \dfrac{\hbar\omega_A}{kT}$ and $U_B = \dfrac{\hbar\omega_B}{kT}$

For the harmonic oscillator, the following equalities $\omega_H = \omega_D\sqrt{2} = \omega_T\sqrt{3}$ are valid. Hence, by calculating separation factors for H-T, H-D, and D-T mixtures and their temperature dependencies one requires only ω value, which can be found from a single α value determined experimentally for any mixture.

When performing the quantum-statistical calculations of the thermodynamic isotope effects, it is useful to use the β-factor introduced by Warshawskii and Waysberg (16), representing an equilibrium constant of an isotope exchange reaction between a molecule and an atom. For a hydride phase, the β-factor is equal to the equilibrium constant of the following reaction:

$$A(Me) + B^{\bullet} \Leftrightarrow B(Me) + A^{\bullet} \tag{13}$$

defined as

$$K = \frac{Z_{B(Me)}Z_{A^{\bullet}}}{Z_{A(Me)}Z_{B^{\bullet}}} \tag{14}$$

and can be expressed as follows:

$$\beta_{Me(A-B)} = (m_A/m_B)^{3/2}\left[\frac{\sinh(u_A/2)}{\sinh(u_A/2(m_B/m_A)^{1/2})}\right]^3 \tag{15}$$

MARCEL DEKKER, INC.
270 Madison Avenue, New York, New York 10016

where $m_A/m_B = Z_A/Z_B$ is the ratio of atom masses of the light and the heavy hydrogen isotopes.

For any isotope pair of molecular hydrogen there can be considered three values of β-factor, which markedly differ from each other (especially at low temperature): at low content of heavy isotope B

$$\beta_{A_2-AB} = \frac{u_{AB}}{u_{A_2}} \frac{\sinh(u_{A_2}/2)}{\sinh(u_{AB}/2)} \tag{16}$$

at high content of heavy isotope

$$\beta_{AB-B_2} = \frac{u_{B_2}}{u_{AB}} \frac{\sinh(u_{AB}/2)}{\sinh(u_{B_2}/2)} \tag{17}$$

at equal content of light and heavy isotopes

$$\beta^0_{A_2-B_2} = \left[\frac{u_{B_2}}{u_{A_2}} \frac{\sinh(u_{A_2}/2)}{\sinh(u_{B_2}/2)}\right]^{1/2} \tag{18}$$

in these expressions $U_{A_2} = \dfrac{\hbar\omega_{A_2}}{kT}$, $U_{AB} = \dfrac{\hbar\omega_{AB}}{kT}$, and $U_{B_2} = \dfrac{\hbar\omega_{B_2}}{kT}$.

The temperature dependencies of β-factor for H-T and D-T mixtures in the range of both low and high content of heavy isotope are shown in Fig.1. Figure 2 shows the dependencies of β-factor on the frequency of local modes $\hbar\omega$ for H-T isotope substitution, which have been computed for the hydride phase by Eq. (15) at 173 and 273 K. As seen, independently of temperature at $\hbar\omega = 0$ $\beta_{Me(A-B)} = 1$. The β value slowly increases with frequency of local modes up to 60 and 80 at $T = 173$ and 273 K, respectively. At higher $\hbar\omega$ values, an abrupt increase of β-fac-

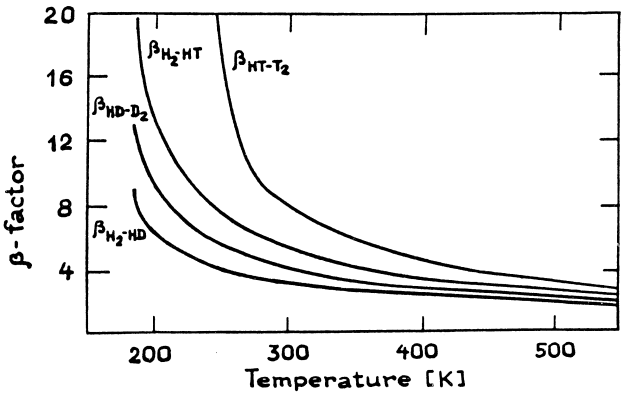

Figure 1. Temperature dependencies of β-factors for molecular hydrogen at H-T ($\beta_{H_2\text{-}HT}$, $\beta_{HT\text{-}T_2}$) and H-D ($\beta_{H_2\text{-}HD}$, $\beta_{HD\text{-}D_2}$) exchanges.

MARCEL DEKKER, INC.
270 Madison Avenue, New York, New York 10016

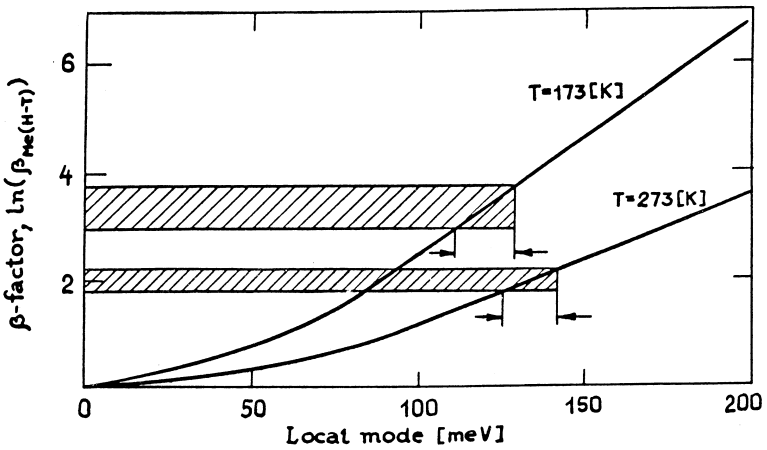

Figure 2. Dependencies of ln $\beta_{Me(H\text{-}T)}$ on energy at $T = 173$ and 273 K.

tor is observed. The range of concentration change of β-factor (whose limits are defined by Eqs. 16 and 17) at 173 and 273 K is shown as shaded areas in Fig. 2. At low $\hbar\omega$ values the heavy isotope is concentrated in the gas phase. At some $\hbar\omega$ value, depending on the temperature and the concentration of isotope under separation, an inversion of the isotope effect is observed. As the result, the gas phase is enriched with the light isotope, i.e., a positive isotope effect will be observed. At $T = 173$ K, the local mode of inversion ranges from 110 (at low tritium concentration) to 130 meV (at high tritium concentration). The local mode of inversion increases with temperature, and at 273 K, it lies between 125 and 145 meV. The difference of ordinates of horizontal straight lines bounding shaded areas is equal to ln α. α versus $\hbar\omega$ dependencies calculated for $T = 273$ K are shown in Fig. 3. The lower curve characterizes isotope effect in the range of low tritium content. The middle curve was obtained for the ratio of isotopes in gas phase of H:T = 1:1. The upper curve corresponds to the high tritium content. The maximal α values at negative isotope effect corresponding to $\hbar\omega = 0$ are equal to the β-factor value of hydrogen (according to Eqs.16 and 17).

Figure 4 shows the dependencies of β-factors of the hydride phase for all pairs of isotopes on the value of reduced temperature $U = \hbar\omega/kT$. The value of β-factor corresponding to the range of temperature and frequencies of harmonic oscillator local mode being of practical interest can be found from these dependencies. Each curve shown in Fig. 4 can be interpreted not only in terms of β-factor vs. ω dependence at $T = \text{const}$ but also as its dependence on $1/T$ at $\omega = \text{const}$. As seen, in a wide temperature range ln β depends linearly on $1/T$. Deviations from the linear dependence are observed only at high temperatures. Note that for

MARCEL DEKKER, INC.
270 Madison Avenue, New York, New York 10016

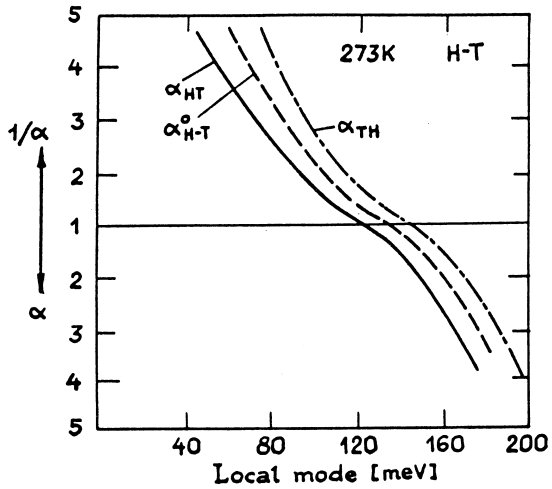

Figure 3. Dependencies of α_{HT}, $\alpha^{o}_{H\text{-}T}$, and α_{TH} on vibrational energy of harmonic oscillator at 273 K.

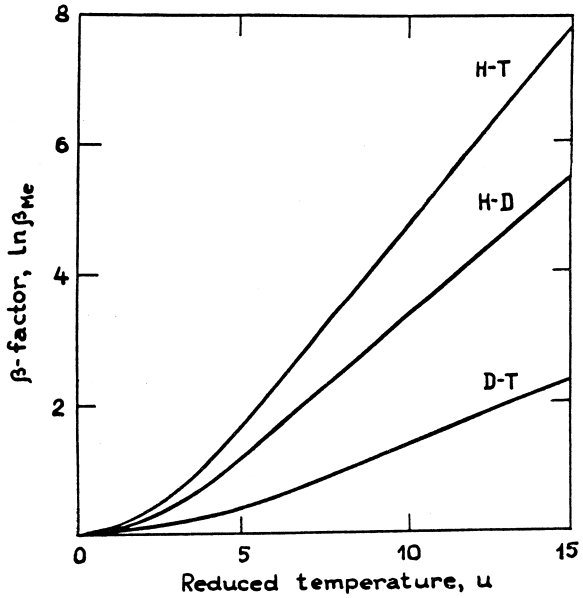

Figure 4. Dependencies of ln $\beta_{Me(H\text{-}T)}$, ln $\beta_{Me(H\text{-}D)}$, and ln$\beta_{Me(D\text{-}T)}$ on reduced temperature *U*.

MARCEL DEKKER, INC.
270 Madison Avenue, New York, New York 10016

the H-T mixture the deviations from linearity are manifested at a lower temperature than for the D-T and H-D mixtures. A decrease of ω values also leads to a decrease of the limiting temperature still corresponding to the linear interval of dependencies shown in Fig. 4.

Let us analyze possible values of separation factor and their temperature dependencies at equilibrium of hydrogen with the hydride phases. Figure 5 shows the temperature dependencies of α_{HD} calculated by Eq. (4) in the range of low heavy isotope content, i.e., corresponding to reaction (9) (14). The highest values of separation factor at the negative isotope effect are limited by the upper curves corresponding to β-factor of hydride phase equal to 1. As seen in Fig. 5, the negative isotope effect decreases with an increase of the local mode up to the inversion.

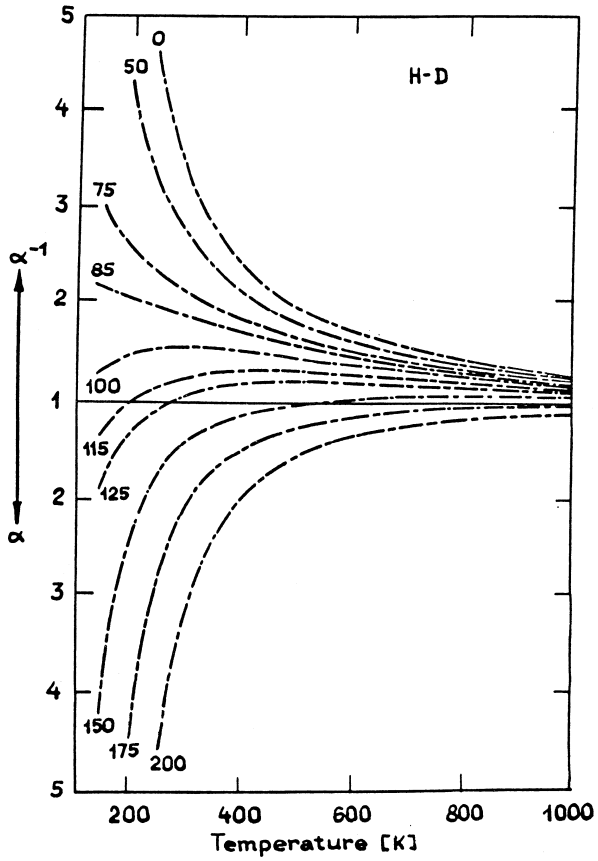

Figure 5. Temperature dependencies of separation factor α_{HD} at different mode energies of hydrogen atom in hydride phase.

MARCEL DEKKER, INC.
270 Madison Avenue, New York, New York 10016

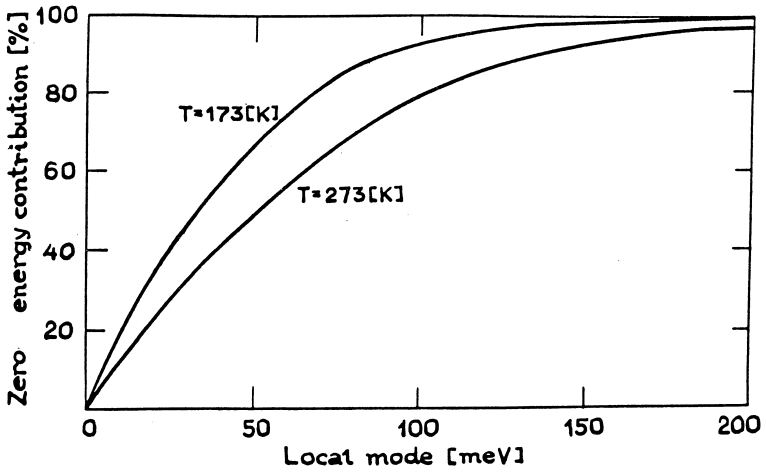

Figure 6. Dependence of zero energy contribution (in %) to $Z_{T(Me)}/Z_{H(Me)}$, or $\beta_{Me(H\text{-}T)}$ values on vibrational energy at $T = 173$ and 273 K.

At the local mode energies of ~100 meV, the temperature dependence of α reveals a maximum that is not typical for the homomolecular isotope exchange (HMIE) reactions. As follows from Fig. 5, the inversion of selectivity can be observed at high temperatures even in systems with considerable positive isotope effect.

The above-performed analysis on the usage of HOM with three degenerated frequencies is useful when computing the sum over states of hydride phase. As it will be shown below, in a number of real systems the energy of an atom in the crystal lattice of hydride phase can be characterized by two or three frequencies of the local modes. In this case, the use of HOM results in the following expressions for β-factor of the hydride phase:

$$\beta_{Me(A-B)} = (m_A/m_B)^{3/2} \prod_{i=1}^{3} \frac{\sinh(u_{A,i}/2)}{\sinh(u_{A,i}/2(m_B/m_A)^{1/2})} \tag{19}$$

As it is follows from Fig. 6, the contribution of excited levels to the sum over states or β-factor of hydrogen atoms in the hydride phase in systems with positive isotope effect at $T \leq 273$ K is low. Hence, the foregoing equations can be simplified. For example, Eq. (12) can be written as follows:

$$Z_{B(Me)}/Z_{A(Me)} = \exp\left(\sum_{i=1}^{3}(u_{A,i} - \mu_{B,i})/2\right) \tag{20}$$

Then, the calculation reduces to determination of the sum over states or β-factor for harmonic oscillator with three degenerated frequencies, whose value is equal to:

$$u_{\mathrm{A}} = \frac{1}{3}\sum_{i=1}^{3} u_{\mathrm{A},i} \tag{21}$$

The two-parameters model, which was also used to calculate isotope effects in the hydrogen-metal systems was described by Malyavskii and associates (17,18). However, a huge amount of information required for calculation by this model makes it inconvenient.

Dependence of Separation Factor on Isotope Concentration

The deviation of equilibrium distribution of isotopes from the equiprobable one in the HMIE reactions causes the dependence of α on concentration (3). In all systems typified by chemical exchange at exchange of hydrogen with molecules of other substances, containing two hydrogen atoms and more, because of a violation of the equiprobable distribution in the HMIE reactions partial compensation of the effect (4,19). In isotope exchange of hydrogen with substance containing only one hydrogen atom and with the hydride phases of metals and IMC, the concentration dependence of α appears to be the strongest.

If the isotope exchange does not proceed by the HMIE reaction mechanism, only limiting α values $\alpha_{\mathrm{A_2–AB}}$ and $\alpha_{\mathrm{AB–B_2}}$ corresponding to the range of low and high content of isotope B, respectively, can be realized in practice. For instance, such a pattern is observed at equilibrium of hydrogen with zeolites, activated carbons, silica gels, and other sorbents for molecular hydrogen (4,7). In all instances, the equilibrium of hydrogen with hydride phases of metals and IMC is followed by dissociation of hydrogen molecules. The HMIE reactions in this case also proceed in the solid surface with the rate, which is, as a rule, several orders of magnitude higher than the rate of interphase isotope exchange (IIE) between gaseous hydrogen and the solid phase. This leads to the concentration dependence of α.

Moreover, even when dissolution of hydrogen isotopes in the solid phase (formation of hydride phases) is not selective (i.e., at $\alpha^0_{\mathrm{A_2–AB}} = 1$) at either initial or final concentration (representing the most difficult separation tasks), remarkable isotope effects of a different sign but equal by their magnitude must be observed (4,7).

Let us consider a concentration dependence of α corresponding to the positive isotope effect. Equilibrium constants of reactions (9) and (10) can be written, respectively, as follows:

$$K_1 = \frac{[\mathrm{B(Me)}][\mathrm{A_2}]}{[\mathrm{A(Me)}][\mathrm{AB}]} \tag{22}$$

MARCEL DEKKER, INC.
270 Madison Avenue, New York, New York 10016

$$K_2 = \frac{[\mathrm{B(Me)}][\mathrm{AB}]}{[\mathrm{A(Me)}][\mathrm{B_2}]} \tag{23}$$

Separation factors for reactions (9) and (10) equal $\alpha_{AB} = K_1/K_1^{\infty} = 2K_1$, and $\alpha_{BA} = K_2/K_2^{\infty} = K_2/2$, respectively. The HMIE reaction (7) can be derived by subtraction of reaction (9) from reaction (10). Hence, the limiting separation factors in the range of low and high heavy isotope content can be expressed as follows:

$$\alpha_{BA} = \frac{\alpha_{AB} K_{AB}}{4} \tag{24}$$

The relation between limiting separation factors α_{HD} and α_{DH} is considered by Botter (20) for H-D isotope exchange from hydrogen isotope mixtures on the hydride phase of Pd-Pt alloy. The temperature dependence of α_{DH} was computed for the H_2-Pd system by using relation (24) from experimental α_{HD} and K_{HD} values of corresponding HMIE reaction (21).

As follows from the definition of α, the value of separation factor at any isotope composition can be expressed in terms of α_{AB}

$$\alpha_{A-B} = \frac{\alpha_{AB}}{2} \frac{2 + [\mathrm{AB}]/[\mathrm{A_2}]}{2[\mathrm{B_2}]/[\mathrm{AB}] + 1} \tag{25}$$

Considering that

$$\frac{[\mathrm{B_2}]}{[\mathrm{AB}]} = \frac{[\mathrm{AB}]}{K_{AB}[\mathrm{A_2}]} \tag{26}$$

one can derive the following expression for the concentration dependence of α:

$$\alpha_{A-B} = \alpha_{AB} \frac{1 + 2[\mathrm{A_2}]/[\mathrm{AB}]}{4/K_{AB} + 2[\mathrm{A_2}]/[\mathrm{AB}]} \tag{27}$$

This expression describes the simplest special case of α dependence on concentration, which includes equilibrium HMIE reactions in both phases (4,19). In the systems with hydride phases under consideration, the mathematical description of α concentration dependence is substantially simplified due to dissociation of dissolved hydrogen into atoms.

At a given hydrogen isotope composition of the gas phase (e.g., at atomic fraction "y" of isotope B), the ratio of hydrogen isotope species $[A_2]/[AB]$ can be found from the following equation:

$$y\left(\frac{[\mathrm{A_2}]}{[\mathrm{AB}]}\right)^2 - (1/2 - \mathrm{y})\frac{[\mathrm{A_2}]}{[\mathrm{AB}]} - \frac{1 - y}{K_{AB}} = 0 \tag{28}$$

At a given atomic fraction "x" of isotope B in the hydride phase the concentration dependence of α can be presented as follows:

$$\alpha_{A-B} = a_{AB} \frac{1 + (1 - x)/(x\alpha_{AB})}{4/K_{AB} + (1 - x)/(x\alpha_{AB})} \tag{29}$$

MARCEL DEKKER, INC.
270 Madison Avenue, New York, New York 10016

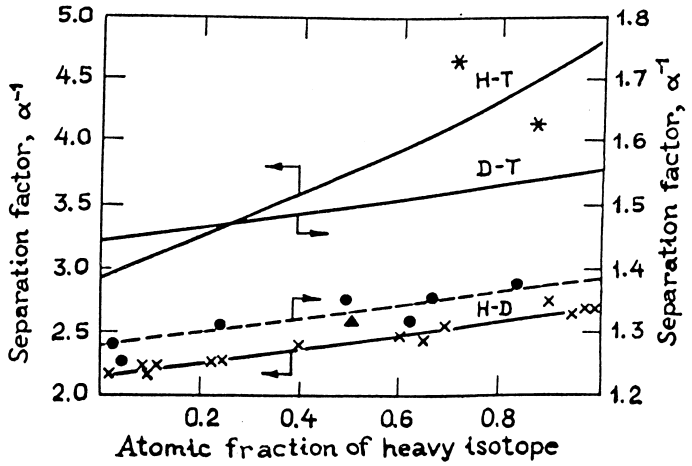

Figure 7. Dependence of separation factors in systems H_2-Pd and H_2-U (dotted lines) on composition of gas phase phase. •, data from Tauabe et al. (28); ▲, Wicke and Nernst (22); ×, data from Andreev et al. (8); *, data from Andreev et al. (27).

The last equation is more convenient as it does not require the solution of square Eq. (28). Since $\alpha_{AB}x/(1 - x) = [AB]/2[A_2]$, Eq. (29) transforms to Eq. (24). According to these relations at a positive isotope effect, α value decreases with heavy isotope concentration. In systems with negative isotope effect (at $\alpha < 1$) an opposite situation is observed. This is an important advantage of such systems when using them for the final concentration of tritium.

A detailed experimental study of α vs. concentration dependencies was performed in the H_2-Pd system known to be characterized by the negative isotope effect. Figure 7 shows the experimental α^{-1}_{H-D} values obtained by Andreev et al. (8) by using the single equilibration technique at equilibrium deuterium content in the gas phase from 2 to 98 at.% and those experimentally obtained (22,23). The linear extrapolation of α^{-1}_{H-D} vs. concentration dependence in the range of low deuterium content gives the limiting value $\alpha^{-1}_{H-D} = 2.16$. This value coincides with those obtained in experiments with hydrogen of the natural isotope composition (24). Concentration dependence of α^{-1}_{H-D} computed with the use of this value by Eq. (27) is shown in Fig. 7 as a solid line. Similar dependencies calculated for H-T and D-T mixtures are also presented in Fig. 7 by solid lines. The following initial data were used for these calculations: $\alpha^{-1}_{HT} = 2.92$ (an average of 3.03 (25) and 2.84 (26)) and $\alpha^{-1}_{DT} = 1.47$ (26). The experimental α_{H-T} values obtained for the H-T mixture at equilibrium concentration of tritium in the gas phase of 89 and 73 at.% at $T = 293$ K (see points) are also shown in Fig. 7 (27). Besides, Fig. 7 presents the experimental data from Tanabe and associates (28,29), and the calcu-

lated curve reported by Andreev et al. (15) for separation factor α_{H-D} at equilibrium of hydrogen with the hydride phase of uranium at $T = 500$–600 K.

For systems with positive isotope effect the concentration dependence of α was studied in the H_2-$LaNi_5$ system for the H-D mixture at $T = 195$ and 273 K and pressure of 0.3 MPa ($n = 6.0$–6.5). The experimental $\alpha_{H\text{-}D}$ values, which have been determined by the single equilibration technique and the computed curves (6,12,30) (solid lines) are presented in Fig. 8. The calculations were performed by using $\alpha_{H\text{-}D}$ values of 1.62 and 1.20 at 195 and 273 K, respectively. An additional series of experiments on determination of $\alpha_{H\text{-}D}$ in the H_2-$SmCo_5$ system was carried out at $T = 273$ K and $P = 0.3$ MPa. The equilibrium composition of hydride phase appeared to be $SmCo_5H_{2.5}$ (30). As it follows from experimental data shown in Fig. 8, both separation factors and their temperature dependencies determined

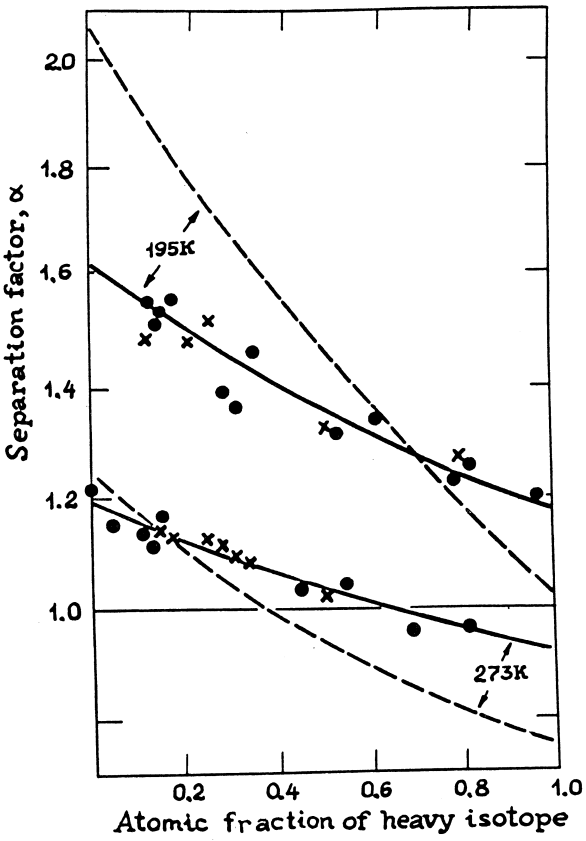

Figure 8. Dependence of separation factors for mixtures H-D (solid line) and H-T (dotted line) in systems H_2-$LaNi_5$ (•) and H_2-$SmCo_5$ (×) on composition of gas phase (7).

MARCEL DEKKER, INC.
270 Madison Avenue, New York, New York 10016

in $LaNi_5$ and $SmCo_5$ IMCs coincide with each other. In the above-mentioned works, the separation factors for the H-T mixture were determined at trace amounts of tritium at $T = 195$ and 273 K and $P = 0.3$ MPa. The α values appeared to equal to 2.10 and 1.25 at 195 and 273 K, respectively. These α_{HT} values were used to compute the concentration dependencies of α_{H-T} presented in Fig. 8 by solid lines.

The following conclusions evidently follow from Figs. 7 and 8: 1) the experimentally determined concentration dependence of α_{H-D} agree well with that calculated by Eq. (27); 2) for the H-T mixture, the dependence is stronger than for the H-D mixture; and 3) at lower temperatures the dependence of α_{A-B} on isotope composition becomes stronger. The last two conclusions are derived from the following facts: in all cases $K_{HT} < K_{HD}$ and both K_{HT} and K_{HD} decrease with decreasing temperature ($K_{HT} = 2.43$ and 1.91, $K_{HD} = 3.19$ and 2.87 at 273 and 195 K, respectively). Concentration dependence of $\alpha_{D\text{-}T}$ is the weakest, since HMIE reaction $D_2 + T_2 = 2DT$ does not result in considerable violation of equiprobable distribution of deuterium and tritium in the molecules involved in this reaction.

In systems with positive isotope effect, a decrease of $\alpha_{A\text{-}B}$ value with an increase of heavy isotope concentration can lead to the inversion of isotope effect. This effect is strongly pronounced in the H_2-$LaNi_5$ system at 273 K where both $\alpha_{H\text{-}T}$ and $\alpha_{H\text{-}D}$ decrease up to 1.

Dependence of Separation Factors on Temperature, Pressure, and Nature of Metals and Intermetallic Compounds

The above-discussed quantum-statistical method for calculation of thermodynamic isotope effects describes well the temperature dependence of the separation factors in hydrogen isotopes-metal hydrides and IMC systems (6,7,31–33). The majority of data available in literature relates to the range of trace tritium contents and low deuterium concentrations. The separation factor describing the reaction of chemical isotope exchange (9) can be expressed by the following equation:

$$\alpha_{AB} = \frac{K}{K^{\infty}} = \frac{u_{A_2}}{u_{AB}} \frac{[(1 - \exp(-u_A))/(1 - \exp(-u_B))]^3}{[(1 - \exp(-u_{A_2}))/(1 - \exp(-u_{AB}))]} \times \frac{[\exp(0.5(u_{A_2} - u_B)]^3}{[\exp(0.5(u_{A_2} - u_{AB})]} \quad (30)$$

The first term in Eq. (30) is constant whereas two others depend on temperature. The temperature dependence of the second term must be considered only at elevated temperatures because at a low temperature it is equal to 1. Hence, the temperature dependence of α_{AB} is determined by the third term reflecting the influence of change of zero energy $\Delta\varepsilon^o$ of hydrogen molecules and atoms on α_{AB} in

MARCEL DEKKER, INC.
270 Madison Avenue, New York, New York 10016

the course of isotope exchange reactions. This makes it possible to simplify the dependence of α_{AB} on temperature as follows:

$$\ln \alpha_{AB} \approx a + b/T \tag{31}$$

where a and b are the constants, which, in turn, can be derived from the known expression connecting equilibrium constant with the Gibbs energy $\Delta G = -\mathrm{RT} \ln \mathrm{K}$ for isotope exchange reaction:

$$-\mathrm{RT} \ln K = \Delta H_{(AB)} - T\Delta S_{(AB)} \tag{32}$$

or

$$\ln \alpha_{AB} = \ln 2 + \frac{\Delta S_{(AB)}}{R} - \frac{\Delta H_{(AB)}}{\mathrm{RT}} \tag{33}$$

Hence, if the experimentally determined temperature dependence of α is adequately described by Eq. (31), the values of thermodynamic parameters of the isotope exchange reaction can be easily calculated. The values of constants a and b for a number of metals and IMC are collected in Table 1. Table 2 presents the available experimental values of separation factors α_{HT} and α_{HD} for hydrogen isotopes-metal hydrides and IMC systems are shown in Table 2.

As seen from Table 2, the major part of experimental data was obtained for the H-T mixture in the range of low tritium concentrations. The main part of data on the H-D mixture was obtained by Aldrich (35) by using a chromatographic technique at a relatively high temperature of 333 K. However, this method enables α values to be determined with lower accuracy than the single equilibration technique.

Based on the data obtained for metal hydrides and IMCs of elements of the third period, Tanaka et al. (36) have attempted to connect α_{HT} value with the number of valence electrons per metal atom $\alpha_{HT} = f(e/m)$. However, the comparative

Table 1. Constants a and b of Temperature Dependence of α_{AB}

Me(IMC)	Temp. Range, K	H-T Exchange		H-D Exchange		Ref.
		a	b	a	b	
Pd(α-phase)	195–350	0.19	−333	0.05*	−214*	(22)
Pd(β-phase)	175–330	−0.30	−284	−0.023	−202	(8)
Ti(hydride)	296–663	0.31	178	—	—	(32)
$TiMn_{1.5}$(α-phase)	213–293	−1.435	537	—	—	(11)
$TiMn_{1.5}$(β-phase)	195–296	−1.02	420	−0.75	295	(31)
$LaNi_5$(β-phase)	223–323	−1.08	357	−0.53	193	(6)
$ZrMn_2$(β-phase)	240–300	—	—	−0.477	240	(34)
$ZrCr_2$(β-phase)	273–373	−1.90	740	−1.5	580	(33)

* Constants a and b were found from experimental sorption isotherms for α^0_{A-B}.

MARCEL DEKKER, INC.
270 Madison Avenue, New York, New York 10016

Table 2. Experimental Values of Separation Factors for Hydrogen Isotopes

Hydrides of Me and IMC	T, K	α_{HT}	$\alpha_{H\text{-}D}$	Ref.
TiH_2	623	0.67	—	(36)
	373	0.45	—	(32)
VH_2	273	1.91	1.73(313 K)	(41)
$CrH_{0.6}$	423	—	0.97*	(42)
$NiH_{0.5}$	298	—	0.92*	(42)
ZrH_2	673	1.07	—	(32)
NbH_2	333.6	—	1.73	(41)
$PdH_{0.4}$	273	0.34	0.46	(8)
UH_3	600	—	0.75	(28)
$TiVH_{4.15}$	313	1.18	—	(36)
$TiCrH_{2.35}$	313	1.54	—	(36)
$TiMnH_{1.99}$	313	1.37	—	(36)
$TiFeH_{1.88}$	273	0.92	—	(36)
$TiCoH_{1.44}$	313	0.85	—	(36)
$TiNiH_{1.44}$	313	0.74	—	(36)
$TiFe_{0.6}Mn_{0.2}H_{1.67}$	313	1.00	—	(36)
$TiMoH_{2.99}$	313	1.61	—	(43)
$ZrCoH_{0.8–1.5}$	473	—	1.14*	(44)
$ZrNiH_3$	300.6	1.05	—	(36)
$TiCr_2H_{1.48}$	273	2.03	—	(36)
$TiCr_2H_{1.68}$	253	2.01	—	(36)
$TiMn_{1.5}H_{2.5}$	195	3.00	1.6(228 K)	(31)
$TiMo_2H_{1.1}$	253	1.87	—	(43)
$TiCrMnH_{1.28}$	273	1.80	—	(36)
$TiCrMnH_{2.19}$	253	2.05	—	(36)
$TiCrMnH_{3.0}$	195	3.25	1.7(228 K)	(7)
$Ti_{0.8}Zr_{0.2}Cr_{1.8}H_{2.8}$	195	3.10	—	(7)
$Ti_{0.8}Zr_{0.2}CrMnH_{2.9}$	195	3.30	—	(7)
$TiMn_{1.4}Ni_{0.1}H_{2.3}$	195	2.80	-	(7)
$ZrV_2H_{4.12}$	273	1.77***	-	
$ZrCr_2H_3$	298	1.90	1.60	(33)
$ZrMn_2H_{0.85}$	300	—	1.38	(34)
$ZrMn_2H_3$	273	1.75***	1.47***	
$Zr_{0.8}Ti_{0.2}Mn_2H_{2.8}$	333	—	1.10	(45)
$LaNi_5H_{6.6}$	195	2.10	1.62	(6)
$MmNi_5H_{6.6}$	273	1.29	—	(36)
$LaCo_5H_{3.4}$	333	—	1.3**	(35)
$MmCo_5H_{2.8}$	333	—	1.2**	(35)
$SmCo_5H_3$	195	2.04	—	(6)
$CaNi_5H_{5.27}$	333	-	1.1**	(35)
$CaNi_5H_{5.5}$	298	-	1.0*	(46)
$LaNi_{4.5}Al_{0.5}H_{5.5}$	333	-	1.2**	(35)
$LaNi_4AlH_{3.8}$	333	—	1.3**	(35)

(continued)

MARCEL DEKKER, INC.
270 Madison Avenue, New York, New York 10016

Table 2. Continued

Hydrides of Me and IMC	T, K	α_{HT}	$\alpha_{H\text{-}D}$	Ref.
$LaNi_4CuH_{5.5}$	195	2.04	—	(30)
$LaNi_4CrH_{4.8}$	195	2.04	—	(30)
$LaNi_4CoH_{5.8}$	333	—	1.1**	(35)
$LaNi_{3.5}Co_{1.5}H_x$	333	—	1.0**	(35)
$LaNi_3Co_2H_{5.0}$	333	—	1.0**	(37)
$LaNi_3Cu_2H_{5.2}$	195	2.04	—	(30)
$LaNi_{2.4}Co_{2.6}H_{5.4}$	333	—	1.1**	(35)
$LaNi_2Co_3H_{4.8}$	333	—	1.1**	(35)
$LaNiCu_4H_{3.5}$	333	—	1.3**	(35)
$LaNiCo_4H_{4.3}$	333	—	1.2**	(35)
$LaNi_{0.5}Co_{4.5}H_{3.9}$	333	—	1.3**	(35)

* Data obtained from isotherms of protium and deuterium sorption.
** Data obtained by chromatographic method.
*** Data of the present work.

analysis of experimental results is complicated because they have been obtained at different temperatures and for the H-D mixture with different concentrations of heavy isotope. For the sake of convenience and comparison, these experimental data have been recalculated for $T = 173$ and 273 K (the most important for isotope separation temperature interval) by using the harmonic oscillator model and concentration dependence of α. Figure 9 shows dependencies $\alpha_{HT} = f(e/m)$ at 173 and 273 K for metals and IMC of the third period elements and dependence $\Delta H_H^{\alpha-\beta} = f(e/m)$. As seen, these dependencies follow an opposite pattern and are characterized by extrema (minimum or maximum) in the same range of e/m values.

Similar dependencies are observed for Zr-based IMC and metals of the third period. The α_{HT} and α_{HD} values determined recently by the single equilibration technique are summarized in Table 3.

The analysis of data collected in Table 3 indicates that α values increase following the change of concentration of electrons per IMC atom from 4 to 5. The maximum α value is observed at $e/m = 5.2$. The further increase of e/m results in decrease of α. IMC phases with concentration of electrons over 6 have low values of α. Compounds of Zr, Ti, and La with transition elements such as, Ni, Co, and Fe fall in this group of IMC. In these compounds hydrogen occupies the tetrahedral positions along with the octahedral ones (37–40), which leads to a decrease of α values. Slight influence of substitution of metal in the compounds of RNi_4Me type is explained by an essentially low effect of metal nature on n_{tet}/n_{oct} ratio and, hence, these IMCs are characterized by close α values.

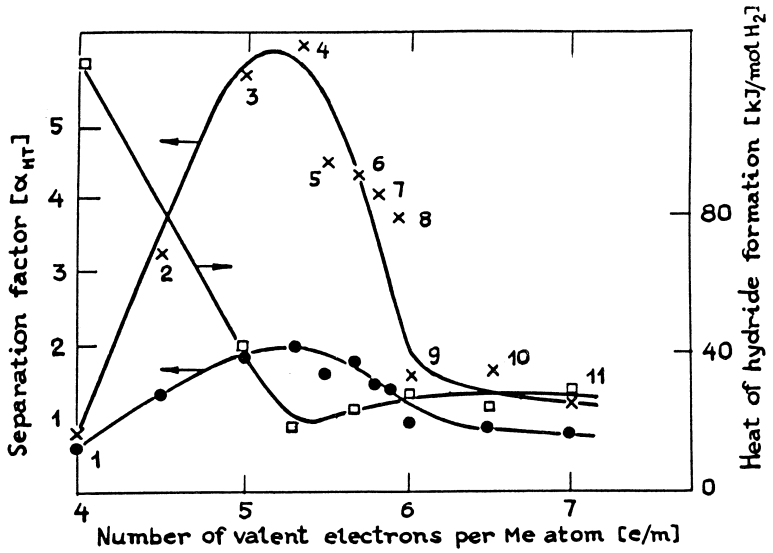

Figure 9. Dependence of separation factors α_{HT} and heat of hydride formation $\Delta H_H^{\alpha\text{-}\beta}$ on number of valence electrons e/m per atom of metal or IMC. (□), $\Delta H_H^{\alpha\text{-}\beta}$; (+), α_{HT} at 173 K; (●). α_{HT} at 273 K; 1, Ti; 2, TiV; 3, TiCr; 4, $TiCr_2$; 5, TiMn; 6, TiCrMn; 7. $TiMn_{1.5}$; 8, $TiMn_{1.4}Ni_{0.1}$; 9, TiFe; 10, TiCo; 11, TiNi.

Table 3. Experimentally Determined Values of Separation Factors α_{AB}

IMC	T, K	α_{HT}	α_{HD}
ZrV_2	250	2.01	—
	298	1.52	—
	298	1.90	1.60
$ZrCr_2$	353	1.35	1.07
	373	1.19	—
$ZrMn_2$	239	2.08	1.66
	296	1.55	1.27
$ZrMn_{2,8}$	250	1.72	1.41
	294	1.41	1.21
$ZrMn_{3,8}$	250	1.69	1.41
	294	1.39	1.19
$ZrMn_2Cr_{0,8}$	250	2.04	1.69
	297	1.54	1.33
ZrMnV	250	1.79	—
	298	1.44	—

Let us consider in detail the temperature dependence of α for hydrides of Pd, U, and $TiMn_{1.5}$ as 1) the experimental data on the local mode frequencies of atoms in the crystalline lattice of these metals are available in the literature; and 2) hydrogen atoms occupy in the lattice only one position (octahedral in Pd and tetrahedral in U and $TiMn_{1.5}$). Let us consider first temperature dependencies of α_{AB}, α_{BA}, and $\alpha^0_{A\text{-}B}$ for H_2-Pd(β-phase) by using the experimental data and the results of quantum-statistical calculations reported by Andreev et al. (8).

The major part of works on the determination of temperature influence on isotope equilibrium was performed with H-D mixture. However, as it follows from Fig. 10, which shows α values determined by different authors, the results obtained scatter dramatically. It is shown by Andreev et al. (8) that the disregarding of concentration dependence of separation factor is the main reason for the result discrepancies. The quantum-statistical calculations of separation factors and their temperature dependence by using Eq. (30) was also reported (8). The values of ω_H and ω_D were found from experimentally determined α^{-1}_{HD} value at $T = 273$ K. These results were substantiated theoretically (47) for $\omega_H/\omega_D = 1.5$, at which the results of calculations on dissolution of protium and deuterium in Pd-β-phase

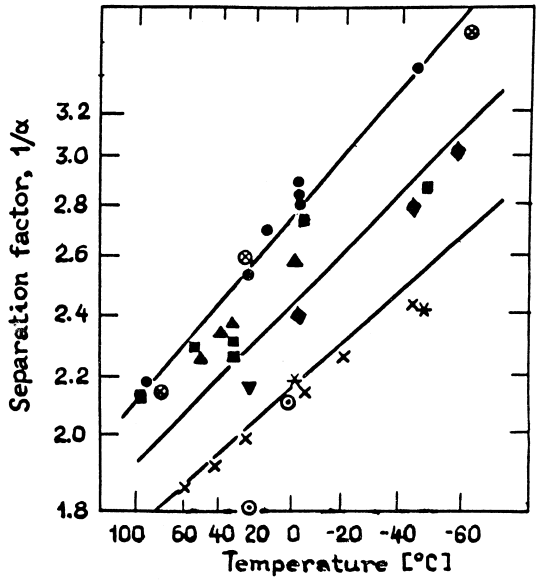

Figure 10. Temperature dependence of separation factor for mixture H-D in system H_2-Pd. (✷,•,◆), data from Andreev et al. (8) at $y \approx 0$, 0.5, and 1; (Δ), data from Wicke and Nernst (22) at $y \approx 0.6$–0.7; (■), data from Domanov et al. (23) at $y \approx 0.5$; (V), data from Glueckauf and Kitt (49) at $y < 0.5$; (×), data from Botter (20) at $y \approx 0$; (⊗, ⊙), chromatographic data from Botter, Glueckauf, and Kitt (20,49).

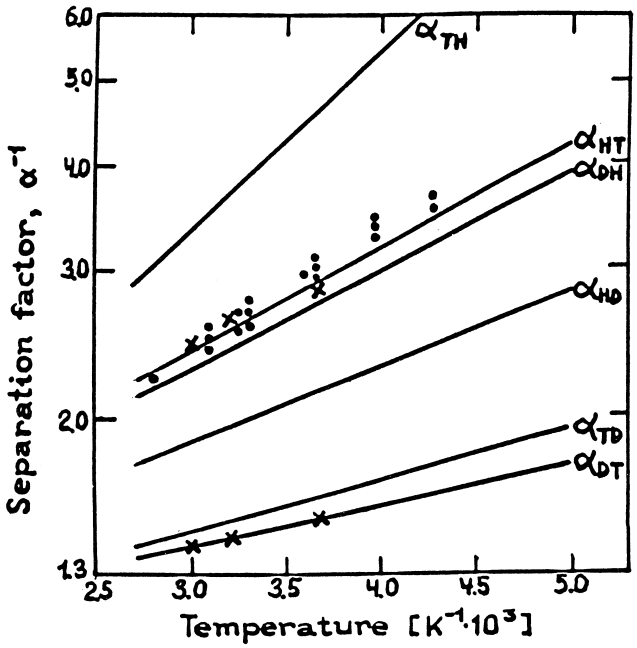

Figure 11. Temperature dependencies of separation factors for binary mixtures of hydrogen isotopes in system H_2-Pd. (•), data from Sicking (10); (×), data from Andreev and Domanov (26).

agreed well with the experimental data (48). The value of $\alpha_{HT}^{-1} = 2.93$ at 273 K was used in determination of ω_T values.

The experimental values of α for H-D and H-T mixtures are shown in Fig. 11. The results of calculations of α_{AB}, α_{BA}, and $\alpha^0_{A\text{-}B}$ vs. temperature dependencies by Eq. (31) using *a* and *b* constants given in Table 1 are also shown in Figs. 10 and 11 by straight lines (8).

As it follows from Figs. 10 and 11, the results of calculations satisfactorily agree with experimental data. A substantial scattering of α values adapted from Wicke and Nernst (22) is explained by the influence of isotope concentration, which is superimposed on the temperature dependence obtained by author.

It is interesting to emphasize a good agreement of the experimental data with the results of calculation performed for the D-T mixture by using α_{HT} and α_{HD} values at 273 K. In all cases the most sharp temperature dependence of α is observed in the range of high concentrations of heavy isotope. The difference in the heats of isotope exchange reactions (which can be easily estimated from slopes of α versus $1/T$ dependencies) in the range of high and low concentration of heavy

isotope results from the heat of HMIE reaction: $H_{(BA)} - H_{(AB)} = H_{AB}$, where H_{AB} is the heat of the HMIE reaction.

A comparison of α values obtained by frontal (20) and displacement chromatography (49) techniques (also shown in Fig. 10) with those determined by the single equilibration method indicates a higher reliability of the last method.

The H_2-Pd system displays an anomalous decrease of the separation factor in the range of trace tritium concentrations (27). This effect dealing with the HMIE reaction can be explained by the change of interaction energy of hydrogen isotopes in the crystalline lattice of metal hydride. The separation factors α_{HT} and α_{DT} shown in Fig. 11 relate to the equilibrium tritium content in the gaseous H-T or D-T mixtures of no less than 10^{-5} at.%. At lower tritium concentration a considerable decrease of α values is observed as it is shown in Fig. 12. The α_{HT} values determined for the tritium content in the initial gas of $\sim 10^{-4}$ at.% (25), which are also shown in Fig. 12, agree well with the data reported by Botter (24).

A similar decrease of α values is observed both for the H-T mixture and the D-T mixture within the whole temperature range studied. Figure 13 shows the temperature dependencies of α_{HT} and α_{DT} obtained at tritium concentrations of 7×10^{-5} and 6.5×10^{-7} at.%, which are characterized by far lower separation factors and heats of the isotope exchange reactions in comparison with the values shown in Fig. 11.

The experimental data on temperature dependence of $\alpha^0_{H\text{-}D}$ in the H_2-UH_3 system and α_{HT} and α_{DT} values for the H_2-$TiMn_{1.5}H_{2.5}$ system are reported (9,11,28,29,31,50,51). As it is shown by Tanabe and associates (28,29), the value

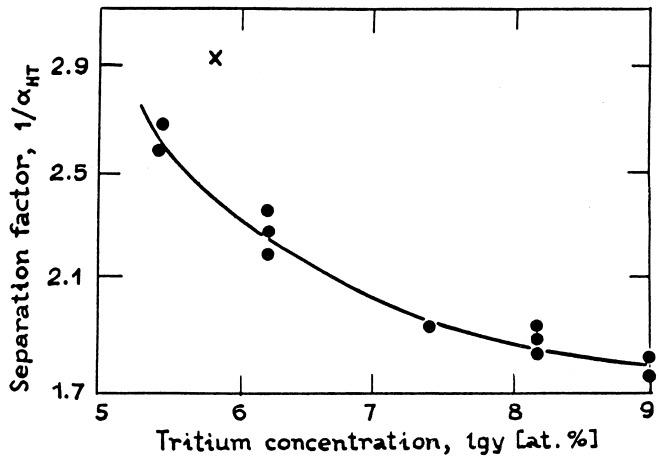

Figure 12. Decrease of α_{HT} at trace tritium contents at 273 K. (•, ×), data from Sicking and Andreev et al. (25,27).

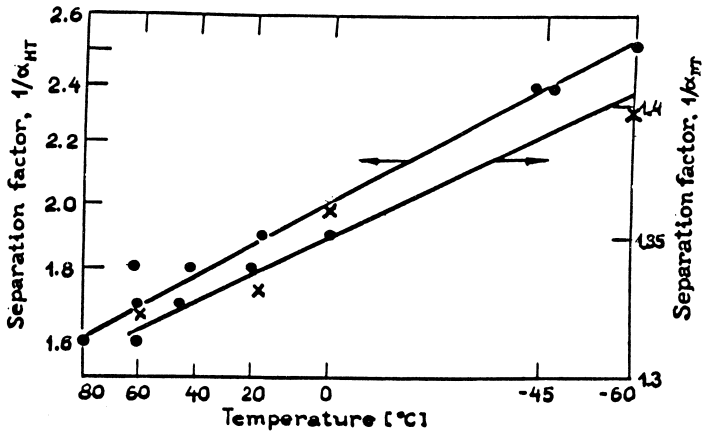

Figure 13. Temperature dependencies of α_{HT} and α_{DT} in system H_2-Pd at $y \approx 7 \times 10^{-5}$ at.% and at $y \approx 6.5 \times 10^{-7}$ at.%, respectively.

of separation factor $\alpha^0_{H\text{-}D}$ in system H_2-UH_3 is essentially independent of temperature in the temperature range from 550 to 670 K and equals 0.75.

This unexpected result can be theoretically justified by means of the harmonic oscillator model. As it follows from the analysis performed by Andreev and Sicking (14), a slight temperature dependence of α is observed in this temperature interval if the frequency of local modes of hydrogen atoms in the crystal lattice is in the range of $100 < \omega_H < 125$ meV (see Fig. 5). It is to be noted that at lower temperatures, namely, 273–373 K, an anomalous temperature dependence of α_{HD} is found to be possible, i.e., α value may increase with temperature.

In the first study of the hydrogen-uranium hydride system, which was carried out by using the neutron scattering method in 1961 (52), the value of $\omega_H = 92$ meV was determined at $T = 77$ K. In subsequent studies (53), the value of $\omega_H = 112$ meV has been found at 300 K, which is essentially closer to the temperature range under study. The calculation by the harmonic oscillator model using $\alpha^0_{H\text{-}D} = 0.75$ at 600 K gives a very close result: $\omega_H = 113$ meV.

Similar to Pd-systems, substantial temperature dependence is also observed for $TiMn_{1.5}$ (9,11,31). Investigation of this system by means of INSS (incoherent neutron scattering spectroscopy) (51) gives for the β-phase of $TiMn_{1.5}$ $\omega_H = 145.8$ meV, which perfectly agrees with the results of calculation by the harmonic oscillator model also giving $\omega_H = 145.8$ meV.

When analyzing the dependence of separation factor on pressure, it is necessary to take into account the composition of solid phase and the positions occupied by hydrogen atoms in the lattice of Me or IMC. In real systems, the situation is complicated by the influence of chemisorbed hydrogen, which can substantially

affect α value at low pressures. This effect is illustrated by data obtained in Pd-H_2 (20,54) and $TiMn_{1.5}$-H_2 systems because they are the most thoroughly studied to date. Figure 14 presents the dependence of separation factors α_{HT} on the fraction of chemisorbed hydrogen φ at 273 K (11,31,51). As seen, the inversion of isotope effect is observed at low hydrogen concentrations in the solid phase that is associated with stronger chemisorption of the heavy isotope. As shown (55), the surface of Pd practically always contains the hydroxyl groups (OH and OD). Investigation of the surface hydrogen by the INSS method (56) gives ω_{Hs} = 101.12 meV. The data on determination of characteristic frequencies −OH on Ni, which is similar to Pd, obtained by the same method demonstrate the presence of two ω values: ω_{O-H}' = 115 meV and ω_{O-H}'' = 400 meV (57). Hence, the energy of chemisorbed protium local modes is essentially higher than the value for local modes in the crystal lattice of Pd that causes the positive isotope effect at

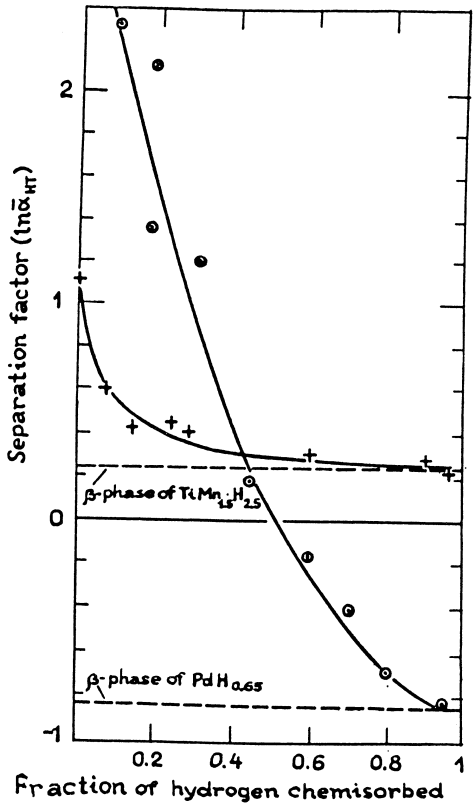

Figure 14. Dependence of separation factor α_{HT} on fraction of chemisorbed hydrogen φ: (⊙), Pd at 353 K; (+), $TiMn_{1.5}$ at 273 K.

MARCEL DEKKER, INC.
270 Madison Avenue, New York, New York 10016

$\omega_H = \sqrt{2}\omega_D = \sqrt{3}\omega_T$. In the H_2-$TiMn_{1.5}$ system, the isotope effects accompanying both adsorption and desorption of hydrogen are positive. As a result, no inversion of the isotope effect is observed (see Fig. 14).

The amounts of chemisorbed hydrogen were determined from deviations from the Siverts law by studying the isotherms of hydrogen sorption in a pressure range from 2.6 to 30 mbar at 253, 273, and 298 K (11). The further investigations corroborated the previous assumption on possible segregation of Ti on the surface of IMC (Ti_3Mn) followed by formation of the surface hydride TiH_x. The presence of the OH groups on titanium surface is confirmed in (11,50,58). The results obtained by studying this system by the INSS method (9,51) show that calculation of α with the use of the harmonic oscillator method gives a good agreement with the experimental data. The α vs. ω dependence is characterized by two peaks revealed in the range of low pressures $P_{H2} < 2$ mbar. The first one observed at $\omega_H = 160$ meV corresponds to the hydrogen atom located in the tetrahedral inter-site of Ti_3Mn and the second peak at $\omega_H = 74$ meV relates to the modes of hydrogen atoms fixed on the OH groups.

Kinetics of Hydrogen Isotopes Interaction with Hydride Phases

Equation of Formal Kinetics

A simple exponential equation is usually used to describe the formal kinetics of isotope exchange reactions. It includes the only constant (rate of exchange R) and is valid in the case of uncomplicated isotope exchange, e.g., occurring in the absence of diffusion deceleration of the transport of exchanging substances to reaction zone and if one of the following conditions is fulfilled:

1. low isotope effect in the system ($\alpha \approx 1$);
2. low concentration of one of the isotopes (x,$y << 1$);
3. low content of one of the reagents (e.g., hydrogen in the gas or the solid phase).

Let us consider a reaction of isotope exchange between hydrogen and a hydride phase of metal or IMC in the general form:

$$A(Me) + AB \Leftrightarrow B(Me) + A_2 \tag{34}$$

Since the rate of isotope exchange is determined by the change of concentration in the gas phase, the kinetic equation can be written in differential form in terms of concentration y:

$$-N_g \frac{dy}{d\tau} = \vec{R}S(1 - x)y - \overleftarrow{R}Sx(1-y) \tag{35}$$

where N_g and N_s are the number of hydrogen moles in the gas and the solid phase, respectively; S is the surface of phases contact (the surface of solid phase); $\vec{R}$ and

Marcel Dekker, Inc.
270 Madison Avenue, New York, New York 10016

$\overleftarrow{R}$ are the rate constants of direct and reverse reaction, mol/(m^{2}sec); F if the degree of exchange $F = (y_0 - y)/(y_0 - y_\infty)$. Integration of Eq. (35) at the above condition 2 leads to the simplest exponential dependence of F on time:

$$-\ln(1 - F) = \vec{R}\, S\left(\frac{1}{N_g} + \frac{1}{\alpha N_s}\right)\tau = \vec{r}\,\tau \tag{36}$$

where r is the observed (experimental) rate constant, s^{-1}.

At low content of heavy isotope B, regardless of the direction of reaction, the dependence $-\ln(1 - F)$ vs. time, τ, is described by a straight line, whose slope depends not only on N_g and N_s but also on α. In the range of high content of heavy isotope (when $\alpha = (1 - y)/(1 - x)$), the kinetic equation transforms to:

$$-\ln(1 - F) = \vec{R}^* S\left(\frac{1}{N_s} + \frac{1}{\alpha N_g}\right)\tau = \vec{r}^*\tau \tag{37}$$

The experimental constants of exchange rate in the range of low and high content of heavy isotope coincide only at $N_g = N_s$. The differences between $\vec{r}$ and $\vec{r}^*$ increase with increasing deviation of ratio N_s/N_g from 1 attaining the maximum value when the change of isotope composition in one of the phases can be disregarded (at $N_g << N_s$ $\vec{r}/\vec{r}^* = \alpha$, and at $N_g >> N_s$ $\vec{r}/\vec{r}^* = \alpha^{-1}$). Hence, the time of half-exchange depends not only on the hydrogen content in contacting phases and α value but also on the change of isotope concentrations.

Finally, at the above condition 3 that is of practical interest only at $N_s >> N_g$ ($x = x_o = x_\infty = \text{const.}$), Eq. (35) transforms to the following relation:

$$-\ln(1 - F) = \frac{\vec{R}\, S\tau(\alpha - \varepsilon x_o)}{\alpha N_g} = \vec{r}\,\tau \tag{38}$$

where $\varepsilon = \alpha - 1$.

Thus, at small amounts of one of the exchanging substances (i.e., hydrogen) not only the value of separation factor but also the amount of gaseous hydrogen in the system and the initial content of isotopes in the hydride phase affect the dependence of F on time. Often in the above kinetic equations, the surface is expressed in terms of specific surface (S_s) and amount of the solid phase g (i.e., $S = S_s g$) or the reaction rate is referred to as the mass unit of the solid phase.

Note that in the above-listed relations, the R value is the rate of direct reaction (34), which is characterized by the positive isotope effect. If a heavy isotope is concentrated in the gas phase (negative isotope effect), reaction (34) must be written as follows: A_2 + B(Me) $\leftrightarrow$ AB + A(Me) and AB + B(Me) $\leftrightarrow$ B_2 + A(Me) for low and high content of heavy isotope B, respectively. Constant $\vec{R}$ standing in Eqs. (36–38) denotes the rate of these reactions in the opposite direction (from the right to the left).

The relations considered describe the kinetics of uncomplicated isotope exchange, when all hydrogen atoms in the hydride phase (as well as in hydrogen

molecules) are identical and the rates of reagents transport to or out of the reaction zone are sufficiently high and do not affect the rate of isotope exchange. However, in many systems with hydride phases of metals and IMC the kinetics of heterogeneous isotope exchange is totally determined by diffusion processes, whose regularities differ from those of formal chemical kinetics because of low diffusivity of hydrogen atoms in the solid phase. The most difficult task arises when differential equations of chemical kinetics and diffusion transport of substance are to be solved simultaneously.

Mass-Transfer of Hydrogen with Hydride Phases

The mass-transfer in systems with solid phase occurs under conditions of constancy of the contact surface, which does not depend on the hydrodynamics of operation mode of apparatus. However, in spite of this fact, the strict description of regularities of mass-transfer in the general case is difficult due to a considerable number of steps of mass-transfer process in the solid phase and strong influence of the quantity of dissolving hydrogen on the rate of diffusion in the solid phase.

It is evident that at isotope exchange of hydrogen, the influence of isotope composition on the parameters of the mass-transfer process can be neglected, i.e., the efficiency of process is assumed to be constant along the height of the separation column. Let us consider the main features of mass-transfer for hydrogen isotope exchange occurring under stationary conditions in separation column and possible ways of its simplification.

Since the rigorous solution of total task of mass-transfer is not obtained so far, we consider the agreed-upon approximation on additive contribution of axial dispersion and mass-exchange processes in the gas and the solid phases in the resistance to mass-transfer (59–61) without the chemical reaction term. In this case one can write:

$$\frac{1}{K_{og}} = \frac{1}{\beta_g} + \frac{1}{m\beta_s} + \frac{D_{eff}}{w^2} \tag{39}$$

where β_g and β_s are the coefficients of mass-exchange in the gas and the solid phases, respectively; K_{og} is the coefficient of mass-transfer in the gas phase; D_{eff} is the effective coefficient of axial diffusion; w is the linear gas velocity; m is the coefficient equal to the tangent of the equilibrium line slope ($m = dx/dy$, where x and y are the isotope concentrations in contacting phases). For the mass-transfer occurring at low concentrations of heavy isotope coefficient m is equal to α.

As follows from Eq. (39), the height of transfer unit (HTU) for the gas phase depends not only on the rate of interphase exchange but also on the intensity of the axial dispersion:

$$h_{og} = h_g + \frac{\lambda\, h_s}{\alpha} + h_{ad} \tag{40}$$

MARCEL DEKKER, INC.
270 Madison Avenue, New York, New York 10016

where $h_g = G_{sp}/\beta_g a_{gr}$, $h_s = L_{sp}/\beta_s a_{gr}$, $h_{ad} = D_{\text{eff}}/w = D_{\text{eff}} S_o \rho / M G_{sp}$, G_{sp}, and L_{sp} are the specific molar flows of gaseous hydrogen and hydrogen dissolved in the solid phase; a_{gr} is the contact surface per unit of the column space; S_o is the fraction of free sectional area of the column; ρ is the gas density; M is the hydrogen molecular mass, and λ is the flows ratio ($\lambda = G_{sp}/L_{sp}$).

The component of HTU corresponding to the axial dispersion depends on the structure of flows in the column. This quantity is responsible for the scale-up effect, which may lead to the rise of HTU when moving from laboratory-scale columns to the industrial ones. Effective coefficient of axial diffusion D_{eff} is used as a quantitative characteristic of the axial dispersion. It depends on the effects of both axial dispersion determined by molecular, turbulent, and convective diffusion and lateral irregularity, which influence decreases with enhancement of the lateral dispersion.

In the columns with fixed solid phase, the last effect is connected with the lateral distribution (profile) of the gas flow rates. Thus, introduction of D_{eff} accounting for all hydrodynamic effects enables to describe within one-dimensional approximation the lateral irregularity as an increase of the axial dispersion (61). It is difficult to calculate D_{eff} value, since it depends not only on the column geometry and operation parameters, such as loading, temperature, pressure, and some others, but also on sizes and shape of solid phase particles, the type of their polydispersity, and even on the method of column filling. That is why the experimental determination of D_{eff} is currently the most reliable. Dependencies of D_{eff} and h_{ad} on the linear gas velocity in the column of diameter 1.5 cm filled with solid phase particles of 2–3 mm size are presented in Fig. 15. The data of Fig. 15 reflect

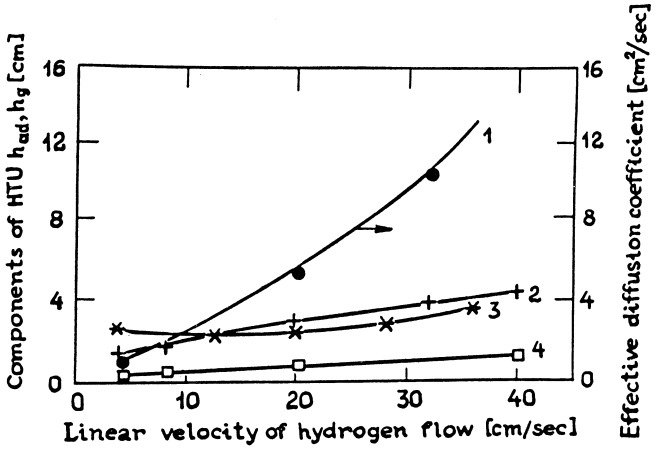

Figure 15. Influence of linear hydrogen flow rate on effective coefficient of axial diffusion (1) and components of HTU h_{ad} at 77 K (3), h_g at 77 K (2) and at 293 K (4) in column filled with spherical sorbent particles of diameter 2.5 mm.

the effect of axial dispersion in the gas phase (hydrogen) on HTU value in a fixed bed column.

The values of D_{eff} were calculated from the experimental curves of response (c-curves) obtained at atmospheric pressure (62). The results of experiments carried out at 77 and 298 K show that D_{eff} does not depend on the temperature at gas velocity $w > 0.04$ m/s. Only at lower gas velocity when D_{eff} slightly exceeds the coefficient of molecular diffusion, the temperature affects the axial dispersion. As seen in Fig. 15, in the column filled with spherical particles of 2–3 mm in diameter HTU = 2–4 mm at $0.01 < w < 0.4$ m/s. As shown by Andreev and associates (62,63), D_{eff} decreases with reduction of particle size and increases at filling the column with particles of irregular shape.

The external diffusion resistance essentially depends on the hydrodynamic pattern of gas flow. When moving from the laminar flow pattern to the turbulent one β_g increases and the contribution of external diffusion resistance reduces. The following equation is usually used for integration of the experimental data on mass-exchange in the range of external diffusion:

$$\text{Nu}_g = A\text{Re}_g\text{Pr}_g^n \tag{41}$$

where A, m, and n are the constants and subscript g denotes gas phase.

The physical properties of hydrogen change over a wide range of temperatures and pressures so that the Prandtl criterion (Pr) is essentially equal to 1. The coefficient m at the laminar flow pattern is close to 0.5 and at the turbulent one it can reach 0.8–0.9 (64,65).

Dependencies of component h_g corresponding to the external diffusion on the rate of hydrogen flow at atmospheric pressure and temperature of 77 and 273 K were computed by using Eq. (41) at $A = 0.725$ and $m = 0.7$ for spherical particles of diameter = 2.5 mm ($S_o = 0.48$). As seen from the dependencies presented in Fig. 15, this component of HTU at 273 K does not exceed 1 mm that is several times less than the diameter of sorbent beads. At 77 K it increases by three to four times primarily due to reduction of the diffusion coefficient reduction by one order of magnitude. Thus, the coefficient of mutual diffusion for H_2-D_2 mixture at 273 and 77 K is equal to 1.13 and 0.116 cm^2/s, respectively. This results in an increase of h_g value reaching at 77 K 4 mm at $w = 0.4$ m/s. The differences in temperature dependence of h_g at G_{sp} = const. appear to be less considerable as at w = const. an increase of G_{sp} by 3.5 times corresponds to a decrease of temperature from 273 to 77 K. A weak dependence of h_g on the column loading (which becomes less remarkable when moving to the turbulent flow pattern) is to be noted.

As it follows from the analysis of Eq. (41), at G_{sp} = const. h_g value does not depend on pressure as D is inversely while ρ is directly proportional to p, and hydrogen viscosity does not practically depend on pressure (e.g., for the change of hydrogen pressure from 0.1 to 10 MPa the viscosity increases only by 2%).

A reduction of the sorbent granule size (d_{gr}) is assumed to result in a decrease of h_g value, which can be more considerable at the laminar pattern of hy-

drogen flow. If the change of the column free space can be disregarded by filling with sorbent of different particle size, h_g is proportional to $d_{\mathrm{gr}}^{2-\mathrm{m}}$.

The main feature of coefficient of the intraparticle mass-exchange β_s consists in independence of its value from the hydrodynamic conditions in the column. Hence, the corresponding HTU component h_s linearly increases with the rise of column loading. The dependence of h_s on G_{sp} is linear and its slope is determined by relation $\lambda/(\alpha\beta_s a_{gr})$, i.e., the dependence of HTU on loading becomes weaker at higher rate of intraparticle mass-transfer or the contact surface. If the size of particles does not affect β_s a reduction of the bead size is to result in proportional decrease of h_s value.

By considering HTU components h_{ad} and h_g we ignored the effect of hydrogen isotope composition on its physical properties, i.e., we assumed these components to be identical for exchange between any hydrogen isotopes. At considerable isotope effects in a system (just such systems are of our interest) it should be taken into account that if heavy isotope is concentrated in the solid phase h_s contribution to HTU for the gas markedly decreases with separation factor. For example, in systems involving IMC phases the h_s contribution is minimal for H-T isotope exchange as $\alpha_{\mathrm{HT}} > \alpha_{\mathrm{HD}} > \alpha_{\mathrm{DT}}$.

By solving the the second Fick's low equation for spherical particles and assuming a linearity of equilibrium equation and the constancy of both concentration on the bead surface and D_e, we obtain the following relation (66):

$$\beta_s^{\circ}\, a_{gr} = \frac{4\pi^2 De}{d_{gr}^2} \tag{42}$$

where D_e is the effective coefficient of diffusion in the sorbent phase.

In spite of a number of rough assumptions, the validity of this expression is corroborated by its use in practice. By accounting for the relation $\beta_s = \beta_s^c E_H$ (here E_H is the hydrogen content in the sorbent, mol/m^3) we obtain:

$$h_s = \frac{G_{sp} d_{gr}^2}{4\pi^2 D_e E_H} \tag{43}$$

The influence of temperature and pressure on h_s value depends on the following parameters: specific properties of the solid phase determining the nature of isotope effect, mechanism and steps of the isotope exchange reaction, intraparticle diffusion affecting the efficiency of mass-transfer and some others.

Dependence of Rate of Isotope Exchange on the Number of Hydrogenation-Dehydrogenation Cycles in the Course of Metals and IMC Activation

Intermetallic compounds produced from the powdered or granulated initial components (metals) require preliminary activation to convert them in a highly ac-

MARCEL DEKKER, INC.
270 Madison Avenue, New York, New York 10016

tive state, in which they are able to easily sorb and desorb hydrogen. The activation process is accompanied by a progressive decrease of IMC particle sizes and, as the result, an increase of specific surface.

The change of the solid phase dispersity in the course of its preliminary activation shows the relation between the particles size or specific surface of the powder and the kinetic parameters of the processes occurring in hydrogen-IMC systems. At the same time, in the works on kinetics of interphase chemical exchange in systems involving hydrogen and IMC hydride phases (67–69) the comparison of kinetics of the process with IMC dispersity data is entirely absent.

The influence of variations of IMC dispersity on the kinetics of reaction of H-T isotope exchange was experimentally examined by Blank et al. (70) for $LaNi_5$ and $Ce_{0.05}La_{0.95}Al_{0.02}Ni_{4.98}$ IMC systems. The experimental $-\ln(1-F)$ vs. τ dependencies (see Eq. 36) obtained at different degrees of preliminary IMC activation are presented in Fig. 16.

As seen from Fig. 16, the curves essentially deviate from straight lines. However, the value of exchange degree F, for which Eq. (36) is valid, increases with the number of sorption acts. A faster "linearization" of the kinetic curves for $Ce_{0.05}La_{0.95}Al_{0.02}Ni_{4.98}$ phase (in comparison with $LaNi_5$) is associated with faster stabilization of the specific surface area for this particular phase as it is shown in Fig. 17. Indeed, the limiting value of S_{sp} for $LaNi_5$ and $Ce_{0.05}La_{0.95}Al_{0.02}Ni_{4.98}$ phases is reached after 8–9 and 1–2 activation cycles, respectively. It has been

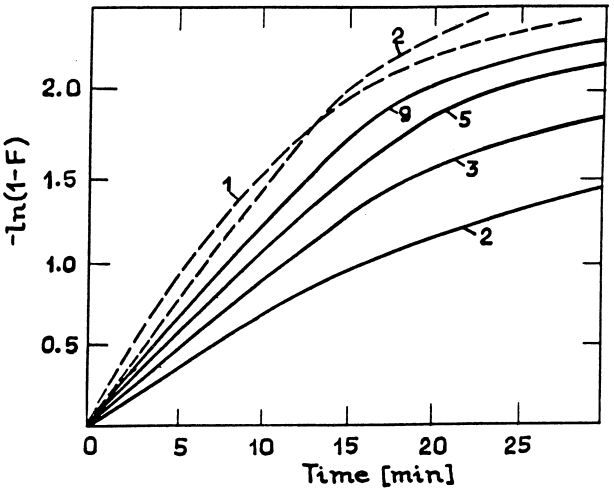

Figure 16. Kinetic curves of hydrogen isotope exchange with $LaNi_5$ hydride (solid line) after 2, 3, 5, and 9 sorption acts and with $Ce_{0.05}La_{0.95}Al_{0.02}Ni_{4.98}$ hydride (dotted line) after 1 and 2 sorption acts at $T = 185$ K and $P = 0.2$ MPa (curve numbers correspond to number of sorption acts).

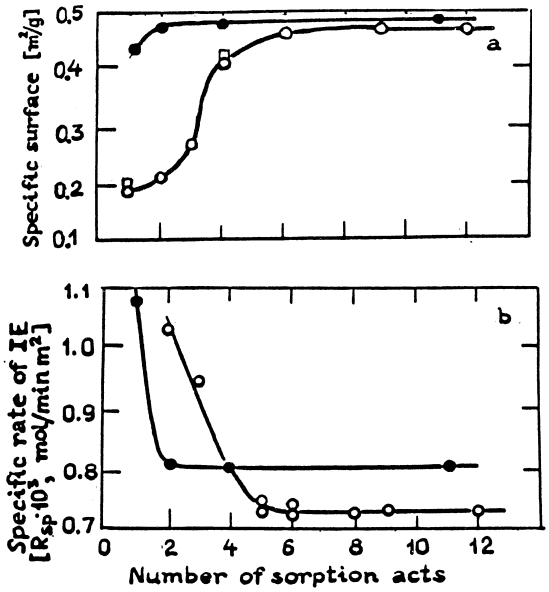

Figure 17. Dependence of specific surface of IMC (a) on number of sorption acts: (o), $LaNi_5$; (□), $LaNi_5H_{6.6}$; (•), $Ce_{0.05}La_{0.95}Al_{0.02}Ni_{4.98}$ and dependence of specific rate constant of isotope exchange R_{sp} (b) at $T = 185$ K and $P = 0.2$ MPa on the number of sorption acts.

found that an increase of IMC surface area in the course of activation occurs only during sorption acts as the S_{sp} values found for hydride phases coincide with the corresponding values determined for dehydrogenated compound at an equal number of sorption acts. As it follows from the results of granulometric analysis, stabilization of size distribution of $LaNi_5$ particles is also observed after ~8 activation cycles.

The limiting values of the particle sizes and specific surface areas were found to strongly depend on the temperature of hydrogenating activation. Thus, for the activation temperatures of 293 and 185 K, the difference in the limiting S_{sp} values exceeds 70%. This fact can be rationalized, since the limiting particles sizes and hence, S_{sp} values are determined (at all other factors being equal) by the value of relative expansion of IMC crystal space at hydrogenation and by the limiting elastic deformation of IMC material. The crystal space expansion increases and the elasticity limit decreases with decreasing temperature. This results in a decrease of the limiting particle size and increases the limiting value of S_{sp}.

Based on the found S_{sp} values (see Fig. 17a), the specific rate constants of the isotope exchange R_{sp} can also be calculated for IMC samples, characterized by

different activation degree (see Fig. 17b). The observed rate constant R is determined from the slope of initial (linear) parts of the kinetic curve.

Separation factors for $LaNi_5$ and $Ce_{0.05}La_{0.95}Al_{0.02}Ni_{4.98}$ have been found to be identical, and their values do not depend on the number of activation cycles and agree well with known literature data obtained for $LaNi_5$.

As it is seen from Fig.18, a remarkable decrease of specific rate constant R_{sp} is observed for both $LaNi_5$ and $Ce_{0.05}La_{0.95}Al_{0.02}Ni_{4.98}$ phases during their preliminary activation. For the latter, the constant R also decreases because of a slight change of S_{sp} value with the number of sorption acts. Let us consider in this context the literature data on the change of surface structure of IMC of $LaNi_5$ type during the preliminary activation. Schlapbach et al. (71–73) have shown that essential segregation is observed for this IMC on the basis of measurement of magnetic susceptibility and electron spectroscopic studies of $LaNi_5$ surface. This effect is more pronounced at higher numbers of sorption acts. As a result, the ratio La:Ni measured on the surface of activated $LaNi_5$ increases to 1:1. This segregation effect is inherent to the majority of IMC and alloys because it is caused by the difference in the surface components of energy. The trend of any system to reach the energy minimum leads to enrichment of the surface with component with lower surface energy. This phenomenon is known as the superficial strain. The stronger the strain, the higher the S_{sp} value or the smaller particle sizes. Hence, an increase of S_{sp} results in a decrease of the surface concentration of the metal with higher surface energy (Ni in IMC under consideration). Segregation on $LaNi_5$ at

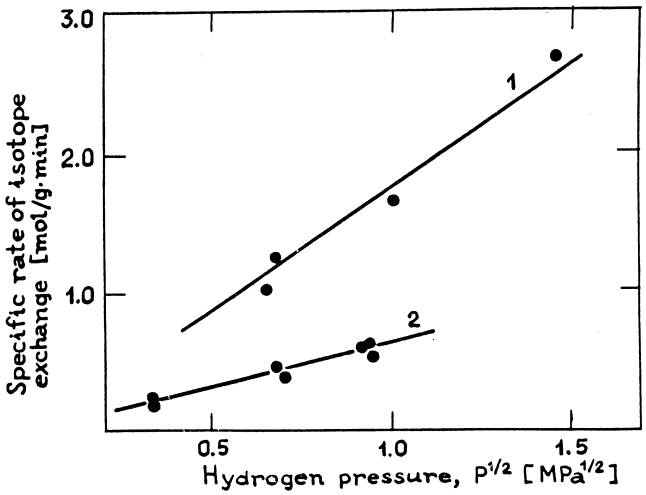

Figure 18. Dependence of isotope exchange rate on hydrogen pressure: 1, TiCrMn; 2, $TiMn_{1.5}$.

low pressures occurs with a sufficiently high rate even at $T = 291$–298 K (71). One can assume that surface concentrations of La and Ni corresponding to the limiting (minimum) particle size are reached at IMC activation in each desorption act (evacuation at elevated temperature).

According to Schlapbach et al. (73), Ni on the surface of $LaNi_5$ is in the form of metallic particles consisting of up to 6000 atoms. Just these particles are responsible for the catalytic activity of $LaNi_5$ surface. It seems evident that all steps of the isotope exchange such as, formation (decay) of activated complexes; diffusion of atomic hydrogen by and through the surface; inclusion of hydrogen in the crystal lattice (outcrops), and some others occur on these particles. Since decrease of Ni content on the IMC surface during activation is followed by a decrease of R_{sp}, one may assume that the rate-determining step of the exchange is associated with the IMC surface.

Influence of Temperature and Pressure on Isotope Exchange Kinetics

Investigation of the influence of temperature and pressure on the rate of isotope exchange in systems involving hydrogen isotopes, metal hydrides, and IMC enables determination of the rate-determining step of the process and ways of its acceleration. The majority of experimental data on influence of temperature and pressure is obtained by the authors with their co-workers for conditions $\alpha \neq 1$ and $x, y << 1$, which corresponds to Eq. (36).

The apparent activation energy of the isotope exchange reaction was found by graphical method from the results of experiments carried out at different temperatures and constant hydrogen pressure. Figure 18 presents the dependence of R on hydrogen pressure. Thermodynamic and kinetic characteristics of hydrogen isotope exchange with some metal hydrides and IMC are collected in Table 4. The results shown in Table 4 were calculated by using the following equation:

$$R = R_o \exp(-E/RT) P^m \tag{44}$$

It should be noted that for all activated metal and IMC samples over a wide range of temperatures and pressures the kinetic equation of the first order (Eq. 36) is valid up to high degrees of exchange ($F \geq 0.8$). This enables determination of R value (characterizing an averaged rate of isotope exchange for particles of different sizes) by the slope of $-\ln(1 - F) = f(\tau)$ dependence. Before consideration of the mechanism of isotope exchange reaction and the analysis of the results shown in Table 4, we dwell on experimental results obtained by different authors who studied isotope exchange in hydrogen-palladium hydride system by static method with forced gas circulation.

The first investigation (74) of both equilibrium and kinetics of isotope exchange in system $H_2(D_2)$-Pd was carried out on granulated palladium with parti-

Marcel Dekker, Inc.
270 Madison Avenue, New York, New York 10016

Table 4. Thermodynamic and Kinetic Characteristics of Interphase Hydrogen Isotope Exchange with IMC Hydrides at $P_{H2} = 0.5$ MPa

IMC Hydride	α_{HT} at 195 K	$R_{HT}10^{-4}$ mol/g min at 195 K	E, kJ/mol	ln R_0	m
$LaNi_5H_{6.6}$	2.12	6.5	17	3.4	0.3
$LaNi_4CuH_{5.5}$	2.12	1.4	28	11.5	0.4
$LaNi_4CrH_{5.0}$	2.12	2.6	27	10.1	0.4
$TiMn_{1.5}H_{2.5}$	3.10	4.1	9.4	−2.0	0.5
$TiMn_{1.4}Ni_{0.1}H_{2.3}$	2.80	8.1	8.5	−1.9	0.5
$TiCrMnH_{0.3}$	3.20	2.1	8.5	−0.9	0.5
$Ti_{0.8}Zr_{0.2}CrMnH_{2.9}$	3.20	2.1	8.5	−0.9	0.5
$Ti_{0.8}Zr_{0.2}Cr_{1.8}H_{2.8}$	3.17	5.3	9.1	−1.9	0.4
$ZrMn_2H_3$	1.75*	27.1*	15.0	0.7	0.4
$ZrCr_2H_3$	2.32*	10.6*	17	0.64	0.5
$ZrV_2H_{4.3}$	1.77*	13.3*	12	−1.2	0.5

* Data obtained at 273 K.

cle size of 2–3 mm. In the temperature range from 273 to 363 K and the pressure range from 35 to 400 mm Hg, the isotope exchange has been shown to be described by Eq. (44) with the following coefficients: $E = 30$ kJ/mol and $m = 1$. In so doing, determination of the dependence of exchange rate on pressure was carried out only at $T = 303$ K. Andreev et al. (74) supposed that in the range of low temperatures the change of the isotope exchange mechanism could be expected. This hypothesis was confirmed later (68,75) by the results obtained from studying the isotope exchange on palladium powder and on aluminium oxide covered with palladium. The experimental data obtained by Andreev et al. (68,75) are presented in Table 5.

The analysis of data given in Table 5 (the value of activation energy, in particular) leads to the conclusion that the intraparticle diffusion is the rate-determining step of the isotope exchange process at low temperatures. In the case of the $Pd/\gamma Al_2O_3$ system, the diffusion of molecular hydrogen in the pores of the carrier is the rate-determining step (75). The influence of diffusion in the gas phase is excluded due to a high rate of hydrogen circulation through the sorbent. Note that in all considered works hydrogen was preliminary purified from nitrogen by low-temperature sorption on activated carbon, from oxygen on reduced Cr-Ni catalyst, and from moisture by sorption on silica gel and zeolites at the temperature of liquid nitrogen.

The study of kinetics of isotope exchange of hydrogen containing traces of tritium on palladium was carried out by Sicking et al. (69). The isotope exchange was studied in the temperature range from 247 to 323 K at a hydrogen pressure of 100 mbar. The activation energy was found to be 11 kJ/mol. Such an essential dif-

Marcel Dekker, Inc.
270 Madison Avenue, New York, New York 10016

ference in activation energies cannot be related to the substitution of deuterium with tritium. This difference can be associated with the purity of hydrogen used in the experiments. For example, hydrogen used by Sicking et al. (69) was of extra high purity. The results obtained in later works (76,77) by using a flow technique combined with the Laser-Raman spectroscopy analysis corroborated the influence of hydrogen purity on activation energy of the isotope exchange reaction. This analytical technique permits determination of the partial pressure of the molecular hydrogen isotope species including the ones containing tritium.

The unit and experimental technique used in the above studies are described by Foltz and Melius (78). The authors concluded that at $P_{H_2(D_2)} = 1050–1200$ torr, $T = 300$ K, and $G = 0.6–1.1$ ml/min, the rate of isotope exchange is determined by the surface processes. Thereafter they suggested a model that adequately describes the ratio H_2:HD:D_2 at the outlet of the reactor. By using a similar technique, Carstens and Encinias (76,77) showed that at $P_{H2(D2)} = 7$ atm in the temperature range from 173 to 299 K at flow $G = 2$ ml/min and at $T > 210$ K, the rate of isotope exchange is determined by the diffusion in the gas phase (at high purity of hydrogen). At lower temperatures, the surface processes become rate-determining, which is confirmed by the influence of CH_4, CO_2, H_2O, and CO impurities on the rate of isotope exchange and the activation energy.

Due to the difference in experimental conditions, the rate constants of isotope exchange reported by different authors cannot be compared with each other. One can only conclude that their values coincide by the order of magnitude. Although the conclusions on the rate-determining step made by different authors are identical, they differently interpret the surface processes. Let us analyze the data obtained on granulated palladium powder and granulated palladium-containing sorbents by using a technique that is described in detail elsewhere (68,79). The influence of temperature, pressure, and loading on the rate of interphase isotope ex-

Table 5. Rates and Activation Energy of Hydrogen Isotope Exchange on Palladium Sorbents

Sorbent	*Dgr*, nm	S_{sp}, m^2/g	T, K	$R_{H\text{-}D}10^7$ mol/m^2s	*E*, kJ/mol
Pd powder	40	10.2	167	0.6	20.5
			175	1.2	
	200	2.5	167	0.7	
			175	1.3	
			195	6.1	21.0
Pd/γAl_2O_3	4	102	195	3.0	
			228	3.0	<2.6
			296	3.0	
Pd/χAl_2O_3	50	7.4	175	1.2	
			195	4.7	18.9

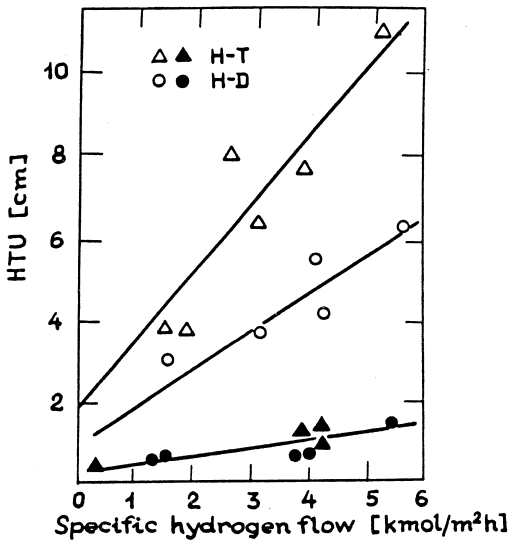

Figure 19. Dependence of HTU (h_{og}) for H-D and H-T mixtures on specific hydrogen flow G_{sp} in H_2-Pd system at $P = 0.5$ MPa, (Δ), H-T; (o), H-D; empty symbols correspond to 195 K, filled symbols to 273 K.

change (IIE) of H-D and H-T mixtures T on granulated palladium (particle size of 0.3–0.5 mm) is reported by Andreev et al. (79). The experimental data obtained were treated by using Eqs. (40) and (41) to find HTU or h_{og} values. Figure 19 shows the dependence of HTU on loading for the gas phase at low temperatures. The results of experiments obtained by studying the dependence of the IIE rate on loading and pressure at high temperatures (293–373 K) show that h_{og} value remains constant ($h_{og} \approx 2$ cm) in the whole range of pressure and loading studied. This fact indicates that diffusion of the gas toward a sorbent surface is the rate-determining factor. This conclusion agrees well with the data reported (77). At low temperatures the activation energy is determined by the slope of $\ln \beta_s a$ versus $1/T$ dependence, which has been found to equal 20.5 kJ/mol for both isotope mixtures.

The results obtained by studying hydrogen isotope exchange on a granulated sorbent consisting of PTFE (polytetrafluoroethylene) and Pd powder ($d_{gr} =$ 1.3 mm) have shown (68) that at low temperatures the exchange kinetics is determined by the transport of hydrogen atoms from the surface into intersites of Pd crystal lattice. At high temperatures the diffusion in pores of the sorbent particles appears to be the rate-determining stage.

Let us revert now to systems involving IMC hydrides. The kinetics of HMIE of hydrogen on hydrides of $LaNi_5$, $Ti_{0.8}Zr_{0.2}CrMn$, CrMn, $ZrMn_2$ was studied (80–82). Literature data on diffusion coefficients of hydrogen atoms in IMC (83)

and on the particle sizes after activation (84–87) make a general analysis of the mechanism of isotope exchange in hydrogen-IMC hydride systems possible. Note that in correctly performed experiments by using a batch technique with forced gas circulation, the deceleration of external diffusion is absent. Taking this into account, let us consider possible rate-determining steps of the IIE process in systems involving hydrogen and IMC hydrides: 1) formation (decay) of activated complex or dissociative adsorption (associative desorption) of hydrogen on IMC surface; 2) migration of hydrogen atoms by the surface (superficial diffusion); 3) conversion from adsorbed to absorbed state and vice versa; 4) diffusion of hydrogen atoms in the crystal lattice of IMC.

Step 1 is common for both HMIE and IIE of hydrogen. The results obtained (80,82) show that at temperatures up to 100 K the mechanism of HMIE reaction, which is followed by the change of activation energy (E), does not vary. The following E values were obtained in the temperature range from 77 to 250 K: E = 6.3, 5.1, and 0.9 kJ/mol for $LaNi_5$, $Ti_{0.8}Zr_{0.2}CrMn$ and $ZrMn_2$, respectively. At equal temperatures, the rate of HMIE is essentially higher than that of IIE. This indicates that the rate of the IIE process cannot be determined by step 1. Step 4 cannot be the rate-determining stage for IMC and Pd.

The results of calculation of the time of half-exchange at low temperatures for a number of IMC and Pd-containing systems are shown in Table 6. As seen from Table 6, the time of half-exchange varies from 0.001 to 50 s depending on the temperature and the size of IMC particles.

Step 2 also cannot be the rate-determining stage because the rate of superficial diffusion is known to be proportional to the gradient of surface hydrogen concentration, which is caused by energetic inequality of different surface regions. An increase of pressure results in filling the most energetically "unfavorable" regions and reduces the gradient of surface concentration, i.e., decreases the process rate. This contradicts the experimentally established fact on increase of R value with pressure. Hence, step 3 is the only one that meets the found kinetic relationships.

Table 6. Estimation of Time of Half-Exchange from Diffusion Coefficient Values

IMC Hydride	E_{act}, kJ/g-at. H	$D_H \times 10^{12}$, m^2/s T = 300 K	$D_H \times 10^{14}$, m^2/s T = 195 K	$\tau_{0.5}$, s T = 300 K	$\tau_{0.5}$, s T = 195 K	$d_{gr} \times 10^6$, m
$PdH_{0,6}$	22.8	54	42	0.0004	0.05	2 (89)
$LaNi_5H_6$	24.0	2.1	1.1	0.3	50	10 (84)
	26.5	5.0	1.5	0.001	0.4	1 (85)
$TiMn_{1,5}$ H_3	21.7	9.8	8.3	0.002	0.3	2 (86)
$Ti_{0,8}Zr_{0,2}$-$CrMnH_3$	21.2	6.2	5.8	0.001	0.1	1 (87)

Isotope Exchange of Hydrogen on Granulated Sorbents

It is well known that an increase of the lattice volume of IMC crystals (up to 25%) accompanying formation of hydrides may cause deformation and even destruction of IMC-made constructions. Formation of fine powders in the course of IMC activation hinders their practical application due to removal of fine particles from apparatuses and a high hydraulic resistance of the fixed powder bed. Preparation of stable granulated IMC-based hydrogen sorbents is particularly important because it provides a high resistance to destruction at multiple hydrogenation and possible thermal and radiation effects. The last is important in the separation of tritium-containing mixtures.

The shaping of IMC powder with polymeric materials (90) is a widely used technique. PTFE was the first binding material used for this purpose (91). However, PTFE-based sorbents decompose at high temperatures (≈450 K) because of interaction IMC components with fluorine (92). Besides, PTFE is the least radiation-resistant polymer (91). Although some polymeric materials, such as polyimides and silicon rubbers, provide rather high thermal and radiation resistance (94,95), insufficient porosity of silicon rubber particles decreases the rate of hydrogen sorption (96). Low thermal conductivity is the common drawback of polymer-based sorbents. Improvement of this property of granulated sorbents can be reached by the use of metals not forming hydrides as a binding component.

A widely used method for preparation of sorbents being resistant to multiple hydrogenation consists of pressing and annealing the powders of partially or completely hydrogenated IMC with powders of Ag, Ni, Cr, Cu, Al, Pb, or their alloys (97–100). However, after five cycles, a decomposition of sorbents is observed. A modified method of Ron et al. (97) enables attaining the resistance of the sorbents. In this case, the powder of activated and totally hydrogenated IMC, whose surface is passivated by means of carbon oxide, is used to prepare the sorbent. After shaping at pressure of 500 MPa and regeneration as described elsewhere (101), the dehydrogenated sorbent contains large pore volume and hence, practically does not change its overall volume by further hydrogenation. After 50 cycles no decline of the sorption-desorption rate is observed (102).

Highly stable porous sorbent withstanding no less than 6000 cycles without destruction can be prepared by mixing activated IMC powder and non-forming hydride metals followed by hydrogenation, and subsequent pressing and simultaneous annealing at a temperature of 370–470 K in hydrogen atmosphere at gas pressure exceeding the pressure of hydride formation. The rate of hydrogen sorption-desorption for such sorbent is considerably higher than that observed for the powdered IMC (99).

The diffusion of hydrogen in pores of granulated sorbent is appended to the above steps of the IIE process. Let us analyze the experimental data, which have been obtained by using granulated sorbents with polymeric binders, such as PTFE

(68) and polyimide (30 mass.%) (63,96,103). Inactivated fine powders (particle size of ~40 μm) of $LaNi_5$ and $Ti_{0.8}Zr_{0.2}CrMn$, which have high thermodynamic (α) and kinetic (*R*) characteristics (see Table 4) were used for preparation of these sorbents.

The sorbents obtained appear to be thermal-resistant up to 673 K, i.e., at a sufficiently high temperature to complete hydrogen desorption. It is also important that interaction of hydrogen with the polymeric binding material does not occur at $T < 673$ K despite the well-known catalytic activity of IMC in hydrogenation and dehydrogenation reactions (104).

As it follows from the results of test-experiments on irradiation of polyimide-based sorbents by using ^{60}Co γ-radiation source (maximal dose power of 5×10^{12} rad/s) at hydrogen pressure of 0.1 MPa and $T = 208$–313 K, the radiation does not remarkably affect the mechanical strength of sorbent (115–121 MPa, which is approximately twice as high as the strength of zeolites).

The results obtained by studying the dependence of IIE efficiency on the specific flow in the column with a diameter of 1 cm at different temperatures for the H-T exchange on the $LaNi_5$-based sorbent at $P_{H2} = 0.5$ [MPa] are presented in Fig. 20. Similar results for the $Ti_{0.8}Zr_{0.2}CrMn$-based sorbent obtained at $P_{H2} = 1.9$ MPa are shown in Fig. 21. As seen from these figures, regardless of temperature, h_{og} depends linearly on the loading at $G_{sp} \leq 4$ mol/m^{2}s for both sorbents.

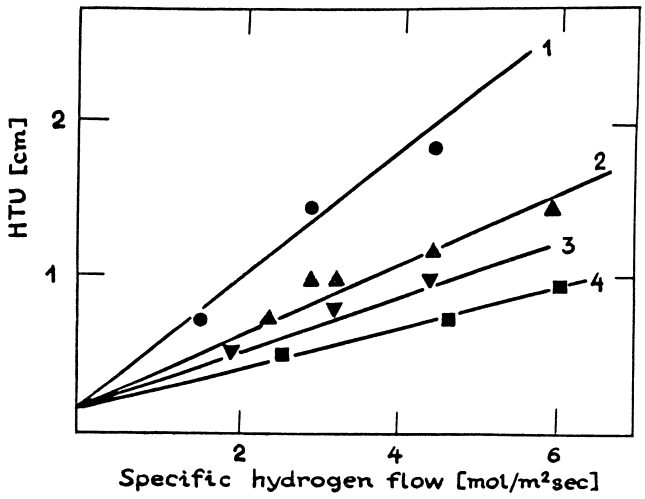

Figure 20. Dependence of h_{og} for H-T mixture on specific hydrogen flow for $LaNi_5$-based sorbent at $P = 0.5$ MPa and different temperatures: 1, 228 K; 2, 250 K; 3, 273 K; 4, 293 K.

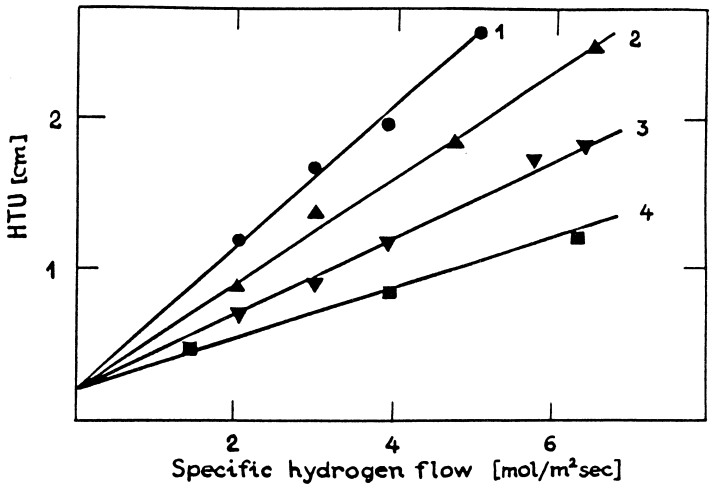

Figure 21. Dependence of h_{og} for H-T mixture on specific hydrogen flow rate for $Ti_{0.8}Zr_{0.2}CrMn$ sorbent at $P = 1.9$ MPa and different temperatures: 1, 195 K; 2, 228 K; 3, 250 K; 4, 273 K.

To explain the experimental dependencies of exchange efficiency on temperature and pressure, let us consider in more detail the components of h_{og} (see Eq. 40), which besides the above-considered factors can also depend on diffusion of molecular hydrogen through the sorbent pores to the active surface of IMC. As it is shown above, the contribution of axial dispersion and external diffusion resistance can be neglected, and hence, basic components of HTU are connected with the diffusion of hydrogen in sorbent pores (h_p) and the transport of hydrogen atoms from the surface to intersites of the crystal lattice (h_m). Hence, Eq. (40) takes the form:

$$h_{og} \approx h_s = h_p + \lambda h_m/\alpha = G_{sp}/(\beta_p a_{gr}) + \lambda L_{sp}/(\alpha\beta_m a_m) \tag{45}$$

where β_p and β_m are the coefficients of mass-exchange processes caused by the diffusion of molecular hydrogen in sorbent pores and by the transport of hydrogen atoms from the surface to intersites of the crystal lattice; a_m is the surface of mass-transfer determined by geometrical surface of the IMC particles (crystallites). For $LaNi_{5-}$ and $Ti_{0.8}Zr_{0.2}CrMn$-based sorbents, $a_m = 5 \times 10^5$ m^2/m^3.

To establish the contribution of each factor in h_{og} one needs to use the data on kinetics of isotope exchange on IMC powders shown in Table 4. The temperature dependence of β_m can be determined from the value of activation energy. The temperature dependence of β_p is determined by the influence of temperature on the coefficient of molecular diffusion $D_{H2.}$ The path of hydrogen molecules $\overline{\lambda}$

at $T = 228$–293 K and $P = 0.5$–1.9 MPa varies from 4.9×10^{-9} to 23.0×10^{-9} m. As $\bar{\lambda}/d_{\text{pore}} << 1$, this corresponds to the range of molecular diffusion, for which $D_{\text{H2}} \sim T^{3/2}$. By using experimental h_{og} values obtained for the H-T mixture at equal loading and solving the sets of Eq. (45), one obtains the following relations for h_p and h_m at $\alpha = \lambda$ (and, hence, for β_p and β_m):

$$\begin{aligned} h_{og1} &= h_{p1} + h_{m1} \quad \text{at} \quad T_1 \\ h_{og2} &= h_{p2} + h_{m2} \quad \text{at} \quad T_2 \end{aligned} \tag{46}$$

The results of calculations, which have been carried out at $G_{sp} = 3$ mol/m^2 s, i.e., at linear dependence of HTU on loading indicating the absence of any influence of hydrodynamic conditions in the column on coefficients β_p and β_m, are shown in Table 7. As seen from Table 7, at $T = 228$ K, the rate of IIE is determined by both the diffusion of molecular hydrogen in the sorbent pores and implantation of hydrogen atoms in the crystal lattice. The value of β_m increases faster with temperature than β_p, and at $T = 228$ K for the $LaNi_5$-based sorbent, the contribution of component h_p to h_{og} value appears to be dominating. For the $LaNi_5$-based sorbent the activation energy is considerably higher than for $Ti_{0.8}Zr_{0.2}CrMn$. Hence, the contribution of h_m to HTU remains essential for the latter sorbent even at moderate temperatures and pressures.

Similar calculations were also carried out for the H-D isotope exchange. For the $LaNi_5$-based sorbent the efficiencies of IIE for both H-T and H-D mixtures are close to each other. For the sorbent on the basis of $Ti_{0.8}Zr_{0.2}CrMn$, the H-T exchange proceeds more effectively than the H-D exchange ($\beta_m^{\text{H-T}} > \beta_m^{\text{H-D}}$).

Table 7. Dependence of h_{og} and β_{og} and Their Components on Temperature and Pressure for H-T Exchange on Granulated Sorbents ($G_{sp} = 3$ mol/m^{2}s)

IMC	P, MPa	T, K	$H_{og}10^2$, m	$\alpha_{\text{H-T}}$	h_m10^2, m	h_p10^2, m	β_{og}, $\frac{\text{mol}}{\text{m}^3\text{s}}$	β_m, $\frac{\text{mol}}{\text{m}^3\text{s}}$	β_p, $\frac{\text{mol}}{\text{m}^3\text{s}}$
	0.5	228	1.43	1.65	0.53	0.90	210	350	340
		250	0.99	1.43	0.20	0.79	300	1100	380
$LaNi_5$		273	0.78	1.27	0.10	0.68	380	2400	440
		290	0.68	1.16	0.06	0.62	440	4300	490
	1.9	228	1.26	1.65	0.39	0.87	240	460	350
		290	0.64	1.16	0.04	0.60	470	6500	500
	1.9	195	1.93	3.30	0.86	1.07	150	100	280
$Ti_{0.8}Zr_{0.2}CrMn$		228	1.39	2.36	0.54	0.85	220	240	350
		250	1.07	2.02	0.33	0.74	280	450	410
		273	0.91	1.77	0.26	0.65	330	650	460
		293	0.81	1.59	0.22	0.59	370	850	500

MARCEL DEKKER, INC.
270 Madison Avenue, New York, New York 10016

It is important to emphasize that coefficient β_p essentially does not depend on 1) the type of isotope mixture (due to the closeness of diffusion coefficients for isotopic species of molecular hydrogen), 2) the IMC nature (due to essentially identical structure of sorbent particles), and 3) pressure. This means that regardless of the above-listed factors at a constant temperature the h_p value is solely determined by the column loading. For example, at $T = 228$ K and $G_{sp} = 3$ mol/m^{2}s, h_p appears to equal 0.85 cm.

Continuous Counter-Current Separation Processes

The main difficulties arising from the practical application of systems with solid phase for isotopes separation deal with the realization of the counter-current movement of the gas and the solid phase. The first variant of the counter-current process was based on the use of columns with compact sorbent bed moving downwards under the action of gravity. Hydrogen moves through the bed in the opposite direction (upwards). The flow-reversal units can also be counter-current. Such counter-current separation processes are often referred to as hypersorption.

Hypersorption

Hypersorption process was originally used to separate H_2-D_2 isotope mixture by sorption of hydrogen on activated carbon (105) and silica gel (106). Thereafter it was realized in the H_2-Pd system for separation of the H_2-HT mixture (107). The column filled with a granulated palladium sorbent (particle size of 1.3 mm) is the main part of the set-up, which is shown schematically in Fig. 22 (4,107). Velocity of the solid phase (palladium hydride) moving downward under action of gravity is controlled by means of a disk machine. The solid phase removed from the disk machine is directed to the bottom container, which works as a desorber. Hydrogen desorption is carried out at $T = 520$–530 K. After desorption, the regenerated sorbent is directed back to the top of the column.

The set-up shown in Fig. 22 can operate by using both the upper section for gas flow reversal (heavy-hydrogen-isotope-concentration mode of operation) and the bottom section for flow reversal (light-isotope-concentration mode of operation). In the first case, the initial mixture of hydrogen isotopes after purification from impurities is fed to the disk machine, passes through the column from the bottom upward, and is sorbed in the top part of the column by regenerated sorbent. Hydrogen desorbed from palladium sorbent in the bottom container is removed from the set-up. In the second case, the sorbent (palladium hydride) loaded with the initial isotope mixture is fed to the column (from the upper container) and all desorbed hydrogen is returned back to the column. The completeness of desorption is controlled by the waste hydrogen flow leaving the unit.

Marcel Dekker, Inc.
270 Madison Avenue, New York, New York 10016

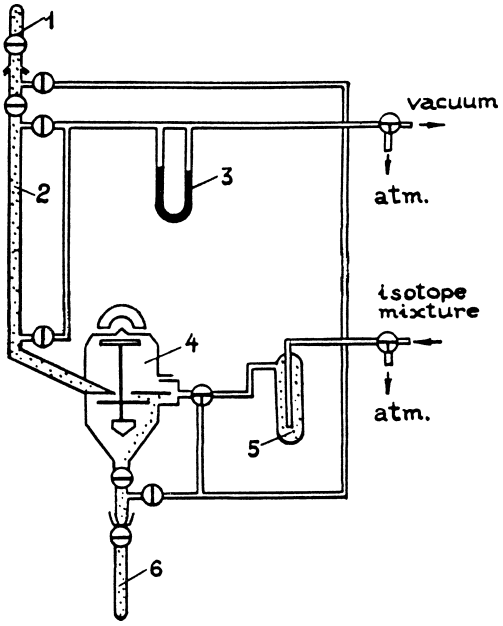

Figure 22. Scheme of experimental hypersorption set-up with granulated palladium sorbent (107): 1, adsorber; 2, separation column; 3, flowmeter; 4, disk machine; 5, purification system; 6, desorber.

The column dimensions, process working parameters, and separation efficiency of the unit are collected in Table 8, where the characteristics of hypersorption separation units using silica gel and activated carbon hydrogen sorbents are also presented. As it follows from the data of Table 8, the highest separation efficiency is observed for the units with palladium-based sorbent.

Table 8. Characteristics of Experimental Hypersorption Set-Ups for Separation of Hydrogen Isotopes

Sorbent	Isotope Mixture	T, K	Loading G_{sp}, kmol/m^{2}h	Column Size, cm		Separation Degree	HETP, cm
				Height	Diam.		
Palladium	H_2-HD	294	1.8	20	1.5	>122*	<2.5
Silica gel	H_2–D_2	77	3 [m/h]**	200	2.0	56***	6.75***
Activated carbon	H_2–D_2	86	2.5–12.6	46	3.8	42	1.6

* Value obtained before achievement of steady state in the column.
** Linear velocity of the sorbent in the column.
*** Values relate to the concentrating part; HETP in the depleting part is equal to 4.75 cm.

Sectional Column

Hypersorption process is characterized by a number of drawbacks (mainly related to the movement of the solid phase), such as sorbent attrition, decrease in separation efficiency due to the axial dispersion in the solid phase, difficulties of sorbent dosage and transport, and some others. For this reason, another version of continuous counter-current separation process in the fixed bed columns was suggested (108) and realized in several variants in a pilot-plant scale. In the proposed method, the counter-current movement of phases is achieved not only through their physical transport but also by the displacement of the flow-reversal section (temperature-zone in the case of thermal desorption) along the immobile bed of the solid phase. The process under consideration is shown schematically in Fig. 23 for a column consisting of several equal sections. Figure 23a refers to the time moment when section 1 operates as a desorber and section 5 is an adsorber. The gas flow passing through sections 2–4 is formed due to elevated hydrogen pressure in the desorber and due to sorption of hydrogen in the adsorber. By passing through the separation sections, the gas exchanges with hydrogen of the solid phase followed by its sorption in section 5. If the column is filled with palladium-based sorbent, the gas phase appears to be enriched with the heavy isotope in the course of isotope exchange with the hydride phase. Once the sorption is completed, the flow-reversal zone displaces upward, i.e., sections 2 and 1 become a desorber and adsorber, respectively, while sections 3–5 comprise the separation zone. As a result, the solid phase *L* "moves" counter-currently against the gas flow *G*. Figure 23a shows a basic scheme of the column operating without product withdrawal. Figures 23b and 23c present the variants of the unclosed modes of operation. Dur-

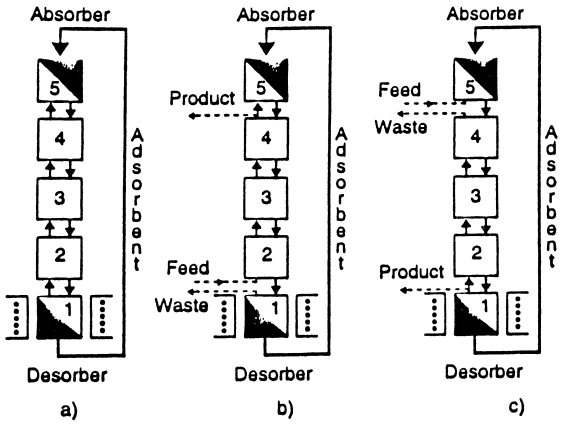

Figure 23. Principle of counter-current "movement" of phases in columns with fixed bed of solid phase (see text).

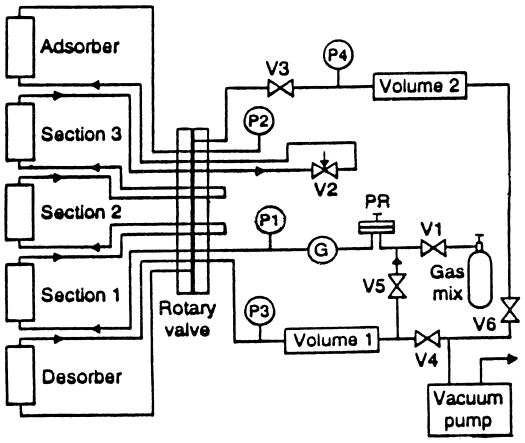

Figure 24. Schematic diagram of experimental set-up (see text).

ing the set-up operation with feed and waste flows, the points of the feed, the product, and the waste withdrawal are to be displaced synchronically along with the above-considered movement of the flow-reversal zone similar to the mode without-product-withdrawal.

In the second variant of the process, the sections separated from each other move counter-currently to the direction of the gas flow. For example, once the gas sorption is completed, section 2 becomes a desorber and section 1 operates as an adsorber due to displacement of sections.

It seems evident that within both variants of counter-current mode of operation, apart from the schemes considered in Fig. 23, it is possible to carry out the separation process in a column with depletion and concentration sections.

The experimental set-up, which has been designed and constructed to test all of the above-mentioned modes of operation, is shown schematically in Fig. 24. The sectional separation column consists of five identical sections, which are packed with granulated palladium adsorbent (75 wt.% Pd and 25% Al). The inner diameter of each section was 11 mm., the height of the bed (h_{bed}) varied in different experiments from 10 to 56 mm. Two sections of the column always served for the flow reversal (as an adsorber and desorber) The other three sections formed the separation zone. The desorber was placed inside of an external heater maintained at the elevated temperature of 493 K. Both the adsorber and the sections in the separation zone were maintained at an operation temperature between 273 and 353K depending on the test purpose.

The sections of the separation column were interconnected with each other as well as with feed and product lines via the specially designed rotary valve con-

sisting of a multichannel disk. The valve was placed in a horizontal position. All sections of the separation column were connected to the rotating part of the valve, whereas the external communication lines were connected to its stationary part. The valve disks were fabricated from stainless steel and were coated with a hard alloy. To avoid a gas leakage through the adjoining surfaces of the disks they were polished and then lubricated with a special radiation-stable lubricant.

The desorber heater and the thermostat for the other column sections were placed on a horizontal platform that was moved down and lifted up each time before and after the rotary valve was actuated. The separation set-up was operating automatically. The gas flow rate in the separation zone was adjusted with needle valve (V2) at the adsorber inlet. The flow was maintained automatically and measured with flowmeter (G). The sections in this zone were kept at a constant pressure by regulator (PR). The pressures in the separation zone (P1), in the adsorber (P2), and in the desorber (P3) were measured with pressure gauges connected to the stationary part of the rotary valve.

Experiments on separation of H-D, H-T, and D-T isotope mixtures were carried out at an atmospheric pressure in a temperature range from 273 to 333 K. The separation degree $K = x_B(1 - x_P)/(x_P(1 - x_B))$ was determined from the isotope composition of the gas at "enriched" (x_B) and "depleted" (x_P) ends of the column after reaching a steady state. Concentration profile in the column was also plotted by average isotope concentrations in the solid phase. Deuterium concentration was determined by spectral technique (from atomic hydrogen spectra) and tritium concentration was measured radiometrically by means of a counter with internal filling.

The main feature of the considered method of counter-current separation is related to a periodic movement (real or relative) of the solid phase. This impairs the separation efficiency of the process as it leads to an increase of HETP value, which was calculated by the experimental data obtained for different heights of the solid phase bed. This dependence was studied for separation of the H-D mixture (see Table 9). As it is seen from Table 9, a 10-fold increase of the bed height of palladium-based sorbent in a section results in an increase of the HETP by a factor of $\sim$7. An overall separation efficiency of the column appeared to be very high. Thus, for the sorbent bed height of 3 cm the maximum separation degree, K, was found to equal 500. The majority of the experiments were carried out in the column with three sections because determination of K value in the column with five sections appeared to be impossible due to very low deuterium concentration at the depleted end of the column (lower than the detection limit of isotope analysis used).

One more interesting result was found, namely, an abrupt impairment of separation efficiency for the H-D mixture on palladium sorbent, which was observed at a deuterium concentration of more than 98 at.%. As seen from Fig. 25, the dependence of HETP on the height of palladium sorbent bed in a section is lin-

MARCEL DEKKER, INC.
270 Madison Avenue, New York, New York 10016

Table 9. Experimental Data on Dependence of Separation Efficiency of H-D Mixture on Height of Palladium Sorbent Bed in Section at $T = 296$ K (108)

Height of Sorbent Bed, cm		Deuterium Concentration, at.%		Separation Degree	HETP, cm
In Section	In Column	x_P	x_B		
1.0	3.0	5.7	96.9	500	0.4
2.0	6.0	2.4	93.3	1566	0.5
5.6	17.0	2.4	97.7	1730	1.2
10.6	37.0	>0.2*	93.5	>15600	2.7

* Detection limit of technique used for isotope analysis.

ear. As it follows from Figs. 26 and 27, in the studied range of separation conditions, HETP does not depend on the loading and temperature in the column at deuterium concentration less than 98 at.%. At higher deuterium contents, the character of HETP dependence on the loading and temperature indicates that under these conditions the separation efficiency is determined by the rate of chemical reaction of hydrogen isotope exchange occurring on the surface of the solid phase.

For comparison the experiments on separation of the H_2-D_2 mixture were carried out in this unit with the use of zeolite NaX as hydrogen sorbent. It is seen from the data presented in Fig. 26 that both on palladium sorbent (at deuterium

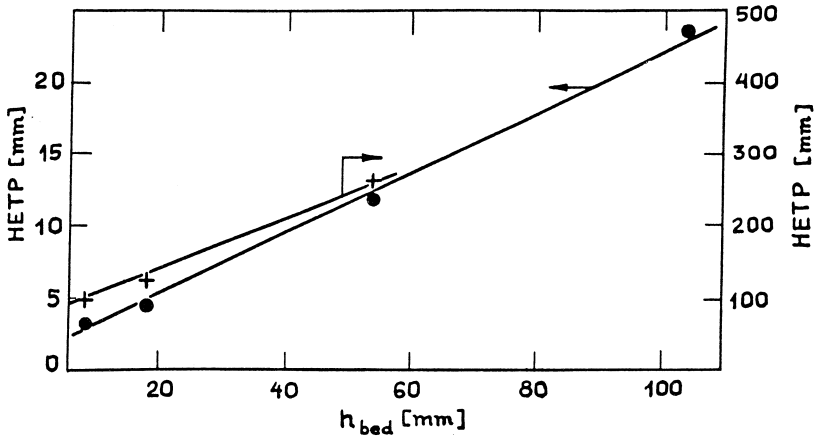

Figure 25. Dependence of HETP on height of palladium sorbent bed in section at $T = 296$ K, $G_{sp} = 1.3$ mol/m^{2}s, and deuterium concentration of: (•), less than 98 at.%; (+), higher than 98 at.% (109,110).

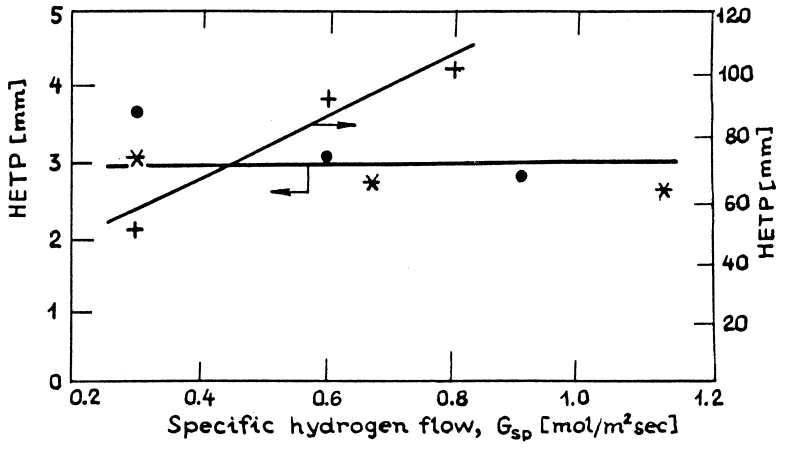

Figure 26. Dependence of HETP on hydrogen flow rate at $T = 296$ K, $H_{bed} = 10$ mm, and deuterium concentration of: (•), less than 98 at.%; (+), higher than 98 at.%; and (*) for zeolite NaX at $T = 78$ K (110).

concentration <98 at%) and on zeolite, the efficiency of mass-transfer is identical, i.e., it does not depend on the sorbent nature.

The results of experiments on separation of mixtures H-T and D-T do not exhibit any unusual features. Indeed, the value of HETP appears to be equal to 3–4

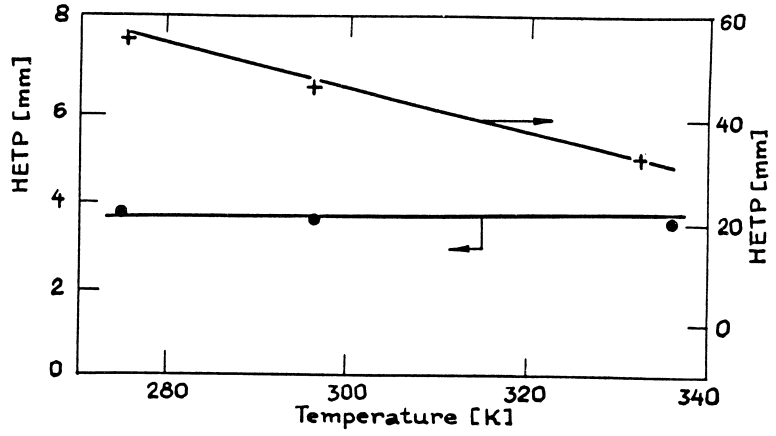

Figure 27. Dependence of HETP on temperature at $H_{bed} = 10$ mm and deuterium concentration of: (•), less than 98 at.% ($G_{sp} = 0.4$ mol/m^{2}s); (+), higher than 98 at.% ($G_{sp} = 0.3$ mol/m^{2}s).

mm, i.e., it is similar to that determined by separation of the H-D mixture at the height of palladium sorbent bed in a section of 10 mm.

The pilot unit comprising a sectional column was recently designed for separation of D-T mixture with high tritium concentration (111). The column consisted of 12 identical sections of 6-cm height each, which were filled with a Pd-based sorbent. A peculiarity of this unit is the storage vessels that allow the operation in a "closed" mode, which does not require control over incoming and effluent flows. This facility permitted processing of up to 4.5 moles of gas per day. The highest tritium concentration obtained with the use of this column was equal to 96%, and its lowest concentration in the remaining mixture was about 0.1%. It was shown that such a counter-current column has a smaller volume than the chromatographic ones when the productivity per palladium mass unit is the same.

Optimum Separation Conditions

The data on isotope equilibrium and efficiency of interphase isotope exchange presented in the previous sections give a possibility to estimate the optimum parameters of the continuous counter-current separation of hydrogen isotopes in systems H_2-Pd and H_2-$LaNi_5$. Since the mass-transfer characteristics, strictly speaking, depend on both the design and dimensions of separation column and on the sorbent characteristics (including the geometrical ones), the approach under consideration and the conclusions resulting from it are more important than the final results of optimization.

The systems with metal or IMC hydride phases are suitable to solve relatively low-scale separation tasks due to lower productivity in comparison with separation processes in gas (vapor)-liquid systems. Let us consider for this reason a separation method based on the use of a column with flow reversal, which is less economically advantageous than a dual-temperature scheme but a simpler one. Let us determine the optimum temperature in separation column (corresponding to the minimal column volume) filled with a granulated sorbent on the basis of $LaNi_5$, which is the system with positive isotope effect.

The height of the sorbent bed in the column depends on the α value, the required separation degree K, the value of relative withdrawal θ, and the h_{og} value (4,60):

$$H_k = h_{og} N_{og} = h_{og}\, \alpha\, \ln((K - \Theta)/(1 - \Theta))/(\alpha - 1) \tag{47}$$

where N_{og} is the number of transfer units (NTU) expressed in terms of driving force for the gas phase. Deriving HTU from Eq. (45) we obtain:

$$H_k = G_{sp} \left(\frac{1}{\beta_p a_{gr}} + \frac{1}{\alpha \beta_m a_m} \right) \alpha\, \ln((K - \Theta)/(1 - \Theta))/(\alpha - 1) \tag{48}$$

MARCEL DEKKER, INC.
270 Madison Avenue, New York, New York 10016

For the unit of productivity P, which is fed with a flow with the initial isotope content y_o, the feed flow depends on the extraction degree ($E = \theta E_m$) as follows:

$$G = P/(y_o \Theta E_m) \tag{49}$$

where E_m is the maximal extraction degree (at $y_o << 1$ $E_m = 1 - 1/\alpha$). The column cross-sectional area, S_k, is expressed as follows:

$$S_k = \frac{G}{G_{sp}} = \frac{P}{G_{sp} y_o \Theta(\alpha - 1/\alpha)} \tag{50}$$

From Eqs. (48) and (50) we obtain that the column volume is equal to:

$$V_k = \frac{P}{y_o \Theta} \ln \frac{K - \Theta}{1 - \Theta} \left[\left(\frac{\alpha}{\alpha - 1} \right)^2 \left(\frac{1}{\beta_p a_{gr}} + \frac{1}{\alpha \beta_m a_m} \right) \right] \tag{51}$$

At definite values of P, y_o, K, and θ, the temperature dependence of V_k is determined by factor.

$$\left(\frac{\alpha}{\alpha - \alpha} \right)^2 \left(\frac{1}{\beta_p a_{gr}} + \frac{1}{\alpha \beta_m a_m} \right)$$

Since this system is not applicable for use at the final concentration stage (due to a decrease of α value), the calculations were performed for the range of initial concentration. As follows from Fig. 28, the optimum temperatures for separation of H-T and H-D mixtures are close to each other and are in the range of 230 to 250 K.

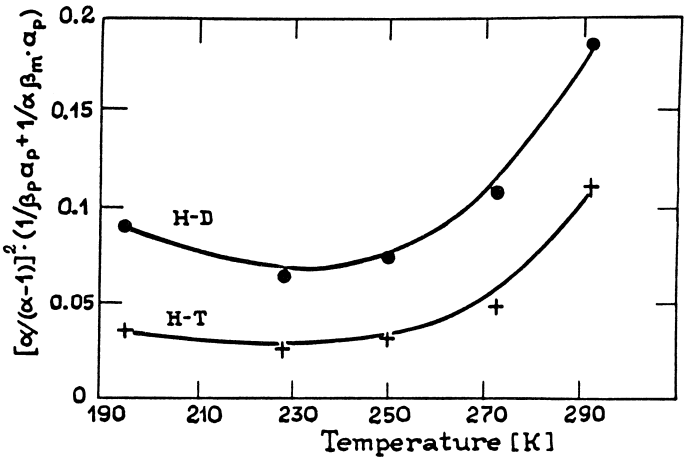

Figure 28. Influence of temperature on volume of counter-current separation column with $LaNi_5$-based granulated sorbent at $P_{H2} = 1.9$ MPa.

MARCEL DEKKER, INC.
270 Madison Avenue, New York, New York 10016

In the H_2-Pd system, the temperature dependence of column volume is less sharp than in the H_2-$LaNi_5$ one. The position of the optimum depends on the size of sorbent particles and lies between 270 and 300 K independently of the mixture being separated (4).

Let us dwell on the choice of column loading. If the impairment of separation efficiency due to the axial dispersion in the gas phase is neglected, the volume of separation part of column remains constant at any loading because of the linear dependence of HTU on loading. In this case, the loading should be increased, since the lower the column diameter, the lower the adverse influence of lateral irregularity.

The axial dispersion at hydrogen passing through the column with fixed bed of different granulated sorbents was studied by the response curves technique (C-curves) to determine the allowable column loading (62). The results obtained have shown that considerable temperature change (from 77 to 300 K) does not affect essentially the axial dispersion. When the column is filled with particles of size of 0.3–1 mm, the gas flow rate cannot exceed 0.2 m/s. For this reason the use of multi-tube columns in plants of high productivity seems to be more advantageous to keep low values of HTU.

The flow-reversal units are important elements of any isotope separation plant. These units are used to provide practically 100% completeness of flow reversal. Incompleteness of flow reversal at the column end enriched with the desired product results in the partial loss of the product. The efficiency of flow-reversal units in systems with hydride phases primarily depends on the character of phase diagram H_2-solid phase and the kinetics of sorption-desorption processes. The completeness of thermal desorption is also determined by the temperature conditions in desorber and the surface area of heat-transfer, which determine the efficacy of its operation.

The width of sorption zone depends on the gas flow rate, the kinetics of sorption (hydrogenation), and the temperature regime. As follows from the results obtained by studying the dynamics of hydrogen sorption (Pd hydrogenation), this process proceeds fast and essentially does not depend on temperature. It is controlled by the molecular diffusion of hydrogen in the pores of sorbent particles (if the heat accompanying the hydride formation is removed effectively). The temperature weakly affects the width of sorption front in comparison with the rate of interphase isotope exchange. Figure 29 shows the results of experiments on dynamics of hydrogen sorption on the Pd-based sorbent obtained by passing the mixture of hydrogen with argon (1:1) through the column. The hydrogen content in the outlet of the column was determined by gas conductivity technique (4).

If the pressure of hydride formation is significantly lower than the operating pressure in the column, the change of the latter in the case of molecular mechanism of hydrogen diffusion in sorbent pores may not essentially influence the width of sorption front. If hydrogen diffusion in the pores proceeds by the Knudsen mechanism, an increase of pressure enhances the mass-transfer. However, the

width of sorption front can also depend on the axial diffusion effect that should be taken into account when calculating the upper flow-reversal unit.

When comparing different hydrogen sorbents, besides the above-considered characteristics (separation factors and HETP), it should be also considered such sorbent properties as volumetric capacity for hydrogen (amount of adsorbed hydrogen per volume unit of sorbent) and the heat of hydrogen sorption (hydride formation) ΔH_H, which affects the energy consumption required for flow reversal.

The main characteristics of systems H_2-Me(IMC), for which the data on the efficiency of mass-transfer are available, are presented in Table 10. System H_2-Pd is characterized by the highest thermodynamic isotope effect. System H_2-$LaNi_5$ is one of the most thoroughly studied. Substitution of pure La by the natural mixture of lanthanides (manufactured in a number of countries) does not change the thermodynamic and mass-transfer characteristics of the system but makes the sorbent less expensive and easily available. The sorbent $Ti_{0.8}Zr_{0.2}CrMn$ belonging to the promising class of compounds of the Laves-phases type is characterized by rather high isotope effect but the required capacity for hydrogen and a high rate of mass-transfer are reached only at elevated pressure.

For comparison, Table 10 also presents the characteristics of the H_2-zeolite NaX system. This system was used in experiments on separation of H-T isotope

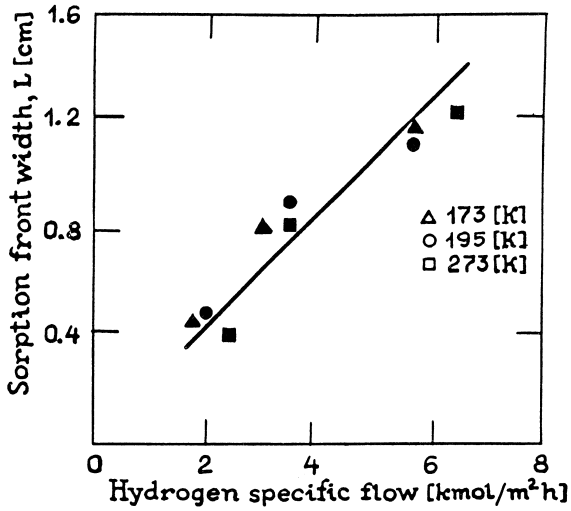

Figure 29. Dependence of width of hydrogen sorption front on specific hydrogen flow in column with diameter of 1 cm filled with granulated palladium sorbent (particle size = 1.3 mm), at $P = 0.05$ MPa.

Table 10. Comparison of Different Working Parameters for Systems with Solid Phase

Sorbent	ΔH_H, kJ/mol	Density of Granulated Bed, g/cm^3	Capacity, cm^{3}H$_2$/g	T, K	α_{HT}	P, MPa	HETP, cm at G_{sp} = 1 mol/m^{2}s
Pd*	41	1.4	50	298	1/2.7	0.1	0.3–0.4
$LaNi_5$**	29	2.0	150	250	1.4	0.5	1.0***
$Ti_{0.8}Zr_{0.2}CrMn$**	—	2.0	—	250	2.0	1.9	1.1***
Zeolite NaX	8.4	0.75	120	77	2.0	0.1	0.3–0.4

* Granulated sorbent (particle size ≈1 mm) containing 75 mass.% of Pd.
** Granulated sorbent (spherical beads with diameter of 1.0–1.5 mm) with 20 mass.% of polymeric binder.
*** Data correspond to G_{sp} = 3 mol/m^{2}s.

mixture in the above-considered set-up with sectional column under conditions, which were similar to those in experiments with the palladium-based sorbent.

The system hydrogen-palladium is characterized by the highest value of separation factors for all binary mixtures of hydrogen isotopes and by the possibility of effective separation at room temperature. It is useful to reemphasize that this system has an important advantage in its use for the final concentration of tritium due to an increase of α^{-1} with concentration of heavy isotope. Although IMC-based sorbents are far less expensive than palladium-based, they are characterized by lower rate of isotope exchange and far less separation factors. Hence, their effective use requires reduced temperature and elevated pressure. Finally, zeolites, which are manufactured world-wide, are the cheapest granulated sorbents. However, low temperature (77 K) is required for effective plant operation, which complicates the equipment and substantially increases both capital and operational costs. Nevertheless, it must be emphasized that despite this drawback, zeolites are characterized by high efficiency of the interphase isotope exchange due to the absence of the steps of molecule dissociation and implantation of atoms into the crystal lattice (which are slow at low temperatures). At the same time, dissociation of hydrogen molecules in hydride forming metals and IMC is followed by the HMIE reactions that allow for extraction of pure isotope in a single column. In the case of zeolites, this reaction is to be performed at an elevated temperature in a special reactor with a catalyst similar to low-temperature rectification of hydrogen.

LIST OF SYMBOLS

Me	hydride-forming metal
θ_H	Einstein characteristic temperature

Marcel Dekker, Inc.
270 Madison Avenue, New York, New York 10016

ω_H	local mode frequency of hydrogen atoms in crystal lattice of metals or IMC
$\hbar$	Planck constant, $\hbar = h/2\pi$
k	Boltzmann constant
U	reduced temperature, $U = \hbar\omega/kT$
N_g, N_s	number of hydrogen moles in gas and solid phases, respectively
F	exchange degree
R	observed rate constant
$\tau_{0.5}$	time of half-exchange
S_0	fraction of free cross-sectional area of column
S	surface area of phases contact; column cross-sectional area
S_{sp}	specific surface of Me or IMC
x_∞,y_∞	equilibrium concentration of heavy isotope in hydride and gas phases, respectively
G	mass of solid phase of Me or IMC
K_{0g}	mass–transfer coefficient for gas phase
β_g, β_s	mass-exchange coefficients in gas and solid phases, respectively
D_{eff}	effective coefficient of axial diffusion
D	coefficient of molecular diffusion of hydrogen
W	linear gas velocity
W_T	velocity of temperature-zone movement
M	slope of equilibrium line ($m = dx/dy$)
H_{0g}, h_{0s}	height of transfer unit (HTU) for gas and solid phases, respectively
H_g, h_s, h_{ad}, h_p	HTU components caused by mass-exchange in gas and solid phase, by axial diffusion in gas, and diffusion in pores, respectively.
G_{sp}, L_{sp}	specific molar flows (molar flow densities) of hydrogen in gas and hydride phase, G_{sp} is also column loading.
λ	flow ratio ($\lambda = G_{sp}/L_{sp}$)
A	contact surface of phases per unit of column volume
M	molecular mass of hydrogen
Nu_g	Nusselt number
Re_g	Reynolds number
Pr_g	Prandtl number
$M_{A,B}$	mass of light or heavy hydrogen isotope
A	light isotope
B	heavy isotope; transition metal
P^A_{H2}	equilibrium pressures determined from sorption isotherm

MARCEL DEKKER, INC.
270 Madison Avenue, New York, New York 10016

P^{D}_{H2}	equilibrium pressures determined from desorption isotherm
x, y	atomic fraction of heavy hydrogen isotope (deuterium or tritium) in hydride and gas phases, respectively
P_1, P_2	equilibrium pressure of pure components over hydride phase
α^{0}_{A-B}	separation factor at equal ratio of isotopes A and B in gas phase
$\alpha_{A-B}, \alpha_{BA}$	separation factors in range of low content of light and heavy isotopes, respectively
$\overline{\alpha}$	effective separation factor
ϕ	fraction of hydrogen atoms retained (sorbed) by α-phase related to overall amount of hydrogen atoms in solid phase in α − β transition range
$K_{A\text{-}B}$	equilibrium constant of reaction of gaseous hydrogen isotope exchange with hydride phases of Me or IMC
K_{AB}	equilibrium constant of homomolecular isotope exchange (HMIE) reaction of hydrogen $A_2 + B_2 \leftrightarrow 2AB$
Z_{A2}, Z_{B2}	partition functions of hydrogen molecules containing light or heavy isotope, respectively
$Z_{A(Me)}, Z_{B(Me)}$	partition functions of hydride phases of metal or IMC including light and heavy hydrogen isotopes, respectively
σ	symmetry number of molecule
m_A, m_B	atomic masses of isotopes A and B, respectively
K	degree of separation
N	number of theoretical plates
N_{0g}, N_{0s}	number of transfer units for gas and solid phases, respectively
R	rate of isotope exchange reaction
d_e	equivalent size of channels in granular bed
μ	gas viscosity
a_m	geometrical surface area of Me or IMC particles per unit volume of column
a_{gr}	geometrical surface area of beads
d_{gr}	diameter of spherical beads
D_e	effective coefficient of hydrogen diffusion in Me or IMC particles
E_H	hydrogen content per unit of sorbent volume
h_e	height equivalent to theoretical plate (HETP)
ξ	form coefficient
Z	height of sorbent bed in column
H	height of separation part of column
θ	relative withdrawal
E, E_m	extraction degree
P	plant productivity
B, P	flows of withdrawal and waste

REFERENCES

1. Basmadjian, D. Can. J. Chem. **1960**, *38*, 149.
2. Kochurikhin, W.E.; Zelvenskii, Ya.D. Zh. Fiz. Khim. **1964**, *38*, 2594. (in Russian)
3. Brodskii, A.I. *Chemistry of Isotopes;* Akad. Nauk SSSR: Moscow, 1957. (in Russian)
4. Andreev, B.M.; Zelvenskii, Ya.D.; Katalnikov, S.G. *Heavy Hydrogen Isotopes in Nuclear Technology;* Energoatomisdat: Moscow, 1987. (in Russian)
5. Bron, J.; Chang, C.F.; Wolfsberg, M. Z. Naturforschung **1972**, *28a*, 129.
6. Andreev, B.; Shitikov, V.; Magomedbekov, E.; Shafiev, A. J. Less-Comm. Met. **1983**, *90*, 161.
7. Andreev, B.M.; Magomedbekov, E.P.; Polevoi, A.S. Tr. Mosk. Khim.-Tekhnol. Inst. im. D.I.Mendeleeva **1984**, *130*, 45. (in Russian)
8. Andreev, B.M.; Polevoi, A.S.; Perevezentsev, A.N. At. Energ. **1978**, *45*, 53. (in Russian)
9. Sicking, G.; Magomedbekov, E.; Hempelmann, R. Ber. Bunsenges. Phys. Chem. **1981**, *85*, 686.
10. Sicking, G. Z. Phys. Chem. **1974**, *53*, 93.
11. Sicking, G.; Magomedbekov, E. In *Met.-Hydrogen Syst*., Proc. Miami Int. Symp., Florida, USA, 1981; Veziroglu, T.N. Ed.; Pergamon Press: Oxford, 1982, 71.
12. Andreev, B.M.; Magomedbekov, E.P.; Shitikov, V.V. At. Energ. **1983**, *55*, 102.
13. Sicking, G. J. Less-comm. Met. **1984**, *101*, 169.
14. Andreev, B.M.; Sicking, G.H. Ber. Bunsenges. Phys. Chem. **1987**, *91*, 177.
15. Andreev, B.M.; Magomedbekov, E.P.; Selivanenko, I.L. At. Energy **1998**, *84*, 132. (in Russian)
16. Warshawskii, Ya.M.; Waysberg, S.E. Zh. Fiz. Khim. **1955**, *29*, 523. (in Russian)
17. Parbuzin, V.S.; Malyavskii, N.I. Zh. Fiz. Khim. **1976**, *50*, 2944. (in Russian)
18. Malyavskii, N.I.; Parbuzin, V.S. Vestn. Mosk. Univ., Ser. Khim. **1977**, *18*, 111. (in Russian)
19. Andreev, B.M.; Zelvenskii, Ya.D.; Katalnikov, S.G.; Uborskii, W.W. Isotopenpraxis **1977**, *12*, 440. (in Russian)
20. Botter, F. J. Phys. Chem. **1965**, *69*, 2485.
21. Botter, F. J. Less-Comm. Met. **1976**, *49*, 111.
22. Wicke, E.; Nernst, G.; Ber. Bunsenges. Phys. Chem. **1964**, *68*, 224.
23. Domanov, M.N.; Andreev, B.M.; Gilburd, S.E. Tr. Mosk. Khim.-Tekhnol. Inst. im. D.I.Mendeleeva **1970**, *67*, 104. (in Russian)

MARCEL DEKKER, INC.
270 Madison Avenue, New York, New York 10016

24. Botter, F. *Isotope Effects in Physical and Chemical Proc.*, Int. Meet., Cluj, Roumania, 1973.
25. Sicking, G. Ber. Bunsenges. Phys. Chem. **1972**, *76*, 790.
26. Andreev, B.M.; Domanov, M.M. Zh. Fiz. Khim. **1975**, *49*, 1258. (in Russian)
27. Andreev, B.M.; Perevezentsev, A.N.; Mandrykin, I.A.; Myasoedov, N.F. Radiokhimia **1986**, *28*, 212. (in Russian)
28. Imoto, S.; Tanabe, T.; Utsunomiya, K. Int. J. Hydr. Energ. **1982**, *7*, 597.
29. Tanabe, T.; Miura, S.; Imoto, S. J. Nucl. Sci. Technol. **1979**, *16*, 690.
30. Andreev, B.M.; Magomedbekov, E.P.; Shititkov, V.V. Zh. Fiz. Khim. **1984**, *58*, 2418. (in Russian)
31. Andreev, B.M.; Dobryanin, O.V.; Magomedbekov, E.P.; Pak, Yu.S.; Shitikov, V.V. Zh. Fiz. Khim. **1982**, *56*, 463. (in Russian)
32. Magomedbekov, E.P.; Andreev, B.M.; Korolev, A.V. Zh. Fiz. Khim. **1990**, *64*, 434. (in Russian)
33. Wedernikova, I.I.; Magomedbekov, E.P.; Andreev, B.M.; Krupentshenko, A.V.; Korolev, A.V. Zh. Fiz. Khim. **1991**, *65*, 1657. (in Russian)
34. Andreev, B.M.; Magomedbekov, E.P.; Rozenkevich, B.M.; Sakharovsky, Y.A. *Heterogeneous reactions of the tritium isotope exchange*, Editorial URSS, Moscow, 1999. (in Russian)
35. Aldridge, F.T. J. Less-Comm. Met. **1985**, *108*, 131.
36. Tanaka, J.; Wiswall, R.H.; Reilly, J.J. Inorg. Chem. **1978**, *17*, 498.
37. Westlake, D.G. J. Less-Comm. Met. **1983**, *91*, 275.
38. Hempelmann, R.; Richter, D; Eckold, G.; Rush, J.J.; Rowe, J.M.; Montoya, M. J. Less-Comm. Met. **1984**, *104*, 1.
39. Westlake, D.G. J. Mat. Sci. **1984**, *19*, 316.
40. Shinar, J.; Shaltiel, D.; Davidov, D.; Grayewski, A. J. Less-Comm. Met. **1978**, *60*, 209.
41. Wiswall, R.H.; Reily, J.J. Inorg. Chem. **1972**, *11*, 1691.
42. Baranowski, B. Metal-hydrogen Systems at High Hydrogen Pressures. In *Hydrogen Metals;* Alefeld, G., Volkl, J., Eds.; Topics Appl. Phys.; Springer-Verlag: Berlin, 1978; Vol. 29, 157.
43. Lunch, J.F.; Reilly, J.J.; Tanaka, J. The Titanium-Molybdenum-Hydrogen System: Isotope Effects, Thermodynamics, and Phase Changes. In *Trans. Met. Hydr.;* Bau, R., Ed.; Amer. Chem. Soc.: Washington, 1978; 342.
44. Devillers, M.; Sirch, M.; Penzhorn, R.D. Z. Phys. Chem. **1989**, *164*, 1355.
45. Jacob, I.; Stern, A.; Moran, A.; Shaltiel, D.; Davidov, D. J. Less-Comm. Met. **1980**, *73*, 369.
46. Sandrock, G.D.; Murray, J.J.; Post, M.L.; Taylor, J.B. Mat. Res. Bull. **1982**, *17*, 887.
47. Bergsma, J.; Goedkoop, J. Physica **1960**, *26*, 744.
48. Boureau, G.; Kleppa, O.; Dantzer, P. J. Chem. Phys. **1976**, *64*, 5247.

MARCEL DEKKER, INC.
270 Madison Avenue, New York, New York 10016

49. Glueckauf, E.; Kitt, G.P. Isotope Separation, In *Proc. Int. Symp*., Amsterdam, 1957; AOC NierNorth Holland Publ. Co.: Amsterdam, 1958; 210.
50. Andreev, B.M.; Magomedbekov, E.P.; Sicking, G.H. *Interaction of Hydrogen Isotopes with Transition Metals and Intermetallic Compounds;* Springer-Verlag: Berlin, 1996.
51. Albers, P. Doctorate thesis, Münster, 1985.
52. Whittemore, W.L.; McReynolds, A.W. *Inelastic Scattering of Neutrons in Solids and Liquids,* IAEA: Vienna, 1961.
53. Rowe, J.M.; Rush, J.J.; Smith, H.G.M.; Flotow, H.E. Phys. Rev. **1976**, *B14*, 3630.
54. Wicke, E.; Brodowski, H. Hydrogen in Palladium Alloys, Hydrogen in Metals. In *Topics Appl. Phys.;* Alefeld, G., Völkl, J., Eds.; Springer-Verlag: Berlin, 1978; Vol. 29, 73.
55. Karas, M.; Magomedbekov, E.P.; Sicking, G.H. J. Less-Comm. Met. **1990**, *159*, 307.
56. Nicol, J.M.; Rush, J.J.; Kelley, R.D. Phys. Rev. **1987**, *B36*, 9315.
57. Renouprez, A.J.; Fouillox, B. J. P. Candy: Surf. Sci. **1979**, *83*, 285.
58. Albers, P.W.; Sicking, G.H.; Ross, D.K. J. Phys. Condens. Matter **1989**, *1*, 6025.
59. Michaels, A.S. Ind. Eng. Chem. **1952**, *44*, 1922.
60. Rozen, A.M. *Theory of Isotope Separation in Columns;* Atomizdat: Moskow, 1960. (in Russian)
61. Rozen, A.M., Ed. *Scaling in Chemical Technology;* Khimiya: Moskow, 1980. (in Russian)
62. Andreev, B.M.; Polevoi, A.S. Izv. Vyssh. Uchebn. Zaved., Khim., Khim. Tekhnol. **1982**, *25*, 889. (in Russian)
63. Andreev, B.M.; Magomedbekov, E.P.; Polevoi, A.S. Tr. Mosk. Khim.-Tekhnol. im. D.I.Mendeleeva **1989**, *156*, 24. (in Russian)
64. Romankov, P.G.; Rashkowskaya, N.B.; Frolov, W.F. *Mass-Transfer Processes in Chemical Industry;* Khimiya: Leningrad, 1975. (in Russian)
65. Aerov, M.E.; Todes, O.M.; Narinskii, D.A. *Apparatures with Immobile Granular Layer;* Khimiya: Leningrad, 1979. (in Russian)
66. Romankov, P.G.; Lepilin, W.N. *Continuous Adsorption of Gases and Vapours;* Khimiya: Leningrad, 1968. (in Russian)
67. Soga, K.; Imamura, H.; Ikeda, S. Nippon Kagaku Kaishi **1977**, *9*, 1304.
68. Andreev, B.M.; Perevezentsev, A.N.; Shitikov, V.V. Zh. Fiz. Khim. **1981**, *55*, 1993. (in Russian)
69. Sicking, G.; Albers, P.; Magomedbekov, E. J.Less-Comm. Met. **1983**, *89*, 373.
70. Blank, K.I.; Magomedbekov, E.P.; Krupentshenko, A.V. Tr. Mosk. Khim.-Tekhnol. Inst. im. D.I.Mendeleeva **1984**, *130*, 80. (in Russian)

MARCEL DEKKER, INC.
270 Madison Avenue, New York, New York 10016

71. Schlapbach, L. J. Phys. F. **1980**, *10*, 2477.
72. Siegman, H.C.; Schlapbach, L.; Brundle, C.R. Phys. Rev. Lett. **1979**, *40*, 785.
73. Schlapbach, L.; Seiler, A.; Stucki, F.; Siegman, H.C. J. Less-Comm.Met. **1980**, *73*, 145.
74. Andreev, B.M.; Boreskov, G.K.; Chang-tsun, C.; Tsionski, V.M. Kinet. Katal. **1966**, *7*, 470. (in Russian)
75. Andreev, B.M.; Perevezentsev, A.N.; Yasenkov, V.I. Zh. Fiz. Khim. **1981**, *55*, 423. (in Russian)
76. Carstens, D.H.W. J. Phys. Chem. **1989**, *164*, 1185.
77. Carstens, D.H.W.; Encinias, P.D. Less-Comm. Met. **1991**, *172–174*, 1331.
78. Foltz, G.W.; Melius, C.F. J. Catal. **1987**, *108*, 409.
79. Andreev, B.M.; Polevoi, A.S.; Petrenik, O.V. At. Energ. **1976**, *40*, 431. (in Russian)
80. Andreev, B.M.; Magomedbekov, E.P.; Pak, Yu.S.; Firer, A.A. Tr. Mosk. Khim.-Tekhnol. Inst. im. D.I.Mendeleeva **1987**, *147*, 59. (in Russian)
81. Jungblut, B.; Sicking, G. J. Phys. Chem. **1989**, *164*, 1177.
82. Blank, K.I.; Magomedbekov, E.P.; Krupentshenko, A.V. Tr. Mosk. Khim.-Tekhnol. Inst. im. D.I.Mendeleeva **1984**, *130*, 70. (in Russian)
83. Hempelmann, R. J. Less-Comm. Met. **1984**, *101*, 69.
84. Belkbir, L.; Gerard, N.; Percheron-Guegan, A.; Achard, J.C. Int. J. Hydrogen Energy **1979**, *4*, 541.
85. Uchida, H.; Uchida, H. Less-Comm. Met. **1983**, *89*, 495.
86. Gamo, T.; Moriwaki, Y.; Yanagihara, N.; Iwaki, T. Less-Comm. Met. **1983**, *89*, 495.
87. Richter, D.; Hempelmann, R.; Vinhas, L.A. J. Less-Comm. Met. **1982**, *88*, 353.
88. Tanaka, S.; Clewley, J.D.; Flanagan, T.B. J.Phys.Chem. **1977**, *81*, 1684.
89. Wicke, E.; Brodowsky, H.; Zuchner, H. *Topics Appl. Phys.;* Springer: Berlin, 1978; Vol. 29.
90. Buhl, H.; Will, S. Sorbent for Hydrogen Storage. US Patent 4,110,425, Int. Cl. CO1B6/24, 1978.
91. Buhl, H.; Will, S. Sorbent for Hydrogen Storage. Patent 2,550,584 BRD, Int. Cl. CO1B6/24, 1977.
92. Batsanov, S.S.; Kapaneva, L.I.; Lasarev, E.V. Zh. Neorg. Chem. **1983**,*28*, 1063. (in Russian)
93. Henley, E.; Johnson, E. *The Chemistry and Physics of High Energy Reactions;* Oxford University Press: Oxford, 1969.
94. Rudman, P.S.; Sandrock, G.D.; Goodel, P.D. J. Less-Comm.Met. **1983**, *89*, 437.
95. Adrova, I.A.; Bessonov, N.I. *Polyimides - a New Class of Heat-Resistant Polymers;* Nauka: Leningrad, 1968. (in Russian)

MARCEL DEKKER, INC.
270 Madison Avenue, New York, New York 10016

96. Andreev, B.M.; Magomedbekov, E.P.; Pak, Yu.S.; Shwedova, G.N. Izv.Vyssh. Uchebn. Zaved., Khim. Khim. Tekhnol. **1986**, *29*, 54. (in Russian)
97. Ron, M.; Gruen, D.; Mendelsohn, M.; Sheft, I. J. Less-Comm.Met. **1980**, *74*, 445.
98. Tusher, E.; Weinzierl, P.; Eder, O. Int. J. Hydr. Energ. **1983**, *8*, 199.
99. Ron, M. Method for Preparing Improved Porous Metal-Hydride compacts and apparatus therefore. UK Patent 2,126,206 Int.Cl. C01B6/24, 1983.
100. Suzuki, Y.; Ogama, Z. Hydrogen Occlusion Material. Patent 59-73401 Japan, Int.Cl. C01B6/24, 1984.
101. Sandrock, G.D.; Goodell, P.D. J. Less-Comm. Met. **1980**, *73*, 61.
102. Suzuki, K.; J. Less-Comm. Met. **1983**, *89*, 183.
103. Andreev, B.M.; Magomedbekov, E.P.; Shwedova, G.N.; Levin, I.N. Zh. Fiz. Khim. **1987**, *61*, 1827. (in Russian)
104. Lezin, Y.S.; Dubinin, M.M. Dokl. Akad. Nauk. SSSR 1**966**, *171*, 382. (in Russian)
105. Basmadjian, D. Can. J. Chem. Engng. **1963**, *Dec*., 269.
106. Clayer, A.; Agneray, L.; Vandenbusche, G.; Petel, P. Z. Anal. Chem. **1968**, *236*, 240.
107. Andreev, B.M.; Polevoi, A.S. Dokl. Akad. Nauk Grus. SSR. **1981**, *7*, 181. (in Russian)
108. Andreev, B.M.; Boreskov, G.K. Zh. Fiz. Khim. **1964**, *38*, 115. (in Russian)
109. Andreev, B.M.; Polevoi, A.S. Zh. Fiz. Khim. **1982**, *56*, 349. (in Russian)
110. Andreev, B.M.; Perevezentsev, A.N.; Selivanenko, I.L. *Isotope Separation and Chemical Exchange Uranium Enrichment*, Proc. Int. Symp., Tokyo, 1990; Fujii, Y., Ishida, T., Takeuchi, K., Eds.; Bull. Research Lab. Nucl. Reactors, 1, 1, 1992.
111. Andreev, B.M.; Selivanenko, I.L.; Golubkov, A.N. Physical Chemical Processes at Selection of Atoms and Molecules, 4th All-Russian (International) Scientific Conference, Moscow, 1999; TSNIIATOMINFORM 1999.

MARCEL DEKKER, INC.
270 Madison Avenue, New York, New York 10016

Request Permission or Order Reprints Instantly!